ISSN 1999-656X

Iraqi Journal of Applied Physics Letters

VOLUME (4) ISSUE (2) APRIL-JUNE 2021

Sponsored and Published by
Iraqi Society for Alternative and Renewable Energy Sources and Techniques

Co-published by
American Quality for Scientific Publishing

IRAQI JOURNAL OF APPLIED PHYSICS LETTERS

The *Iraqi Journal of Applied Physics Letters (IJAPLett)* is a peer reviewed journal of high quality devoted to the publication of original research papers from applied physics and their broad range of applications. IJAPLett publishes quality original research letters in physics and its applications in the broadest sense. It is intended that the journal may act as an interdisciplinary forum for physics and its applications. Innovative applications and material that brings together diverse areas of physics are particularly welcome. IJAPLett aims to disseminate knowledge; provide a learned reference in the field; and establish channels of communication between academic and research experts, policy makers and executives in industry, commerce and investment institutions. IJAPLett is a quarterly specialized periodical dedicated to publishing original letters in: Applied & Nonlinear Optics, Applied Mechanics & Thermodynamics, Digital & Optical Communications, Electronic Materials & Devices, Laser Physics & Applications, Plasma Physics & Applications, Quantum Physics & Spectroscopy, Semiconductors & Optoelectronics, Solid State Physics & Applications, Alternative & Renewable Energy, and Environmental Science & Technology.

ISSN (Print): 1999-656X, ISSN (Online): 2958-6488

EDITORIAL BOARD

Editorial Office:
P. O. Box 55259, Baghdad 12001, IRAQ
Website: www.iraqiphysicsjournal.com
Emails: editor@iraqiphysicsjournal.com, editor_ijap@yahoo.co.uk, ijap.editor@gmail.com,

ADVISORY BOARD

SPONSORED BY
IRAQI SOCIETY FOR ALTERNATIVE AND RENEWABLE ENERGY SOURCES AND TECHNIQUES (I.S.A.R.E.S.T.)
P. O. Box 55259, Baghdad 12001, IRAQ

PUBLISHED BY
AMERICAN QUALITY FOR SCIENTIFIC PUBLISHING INC.
1479 South De Gaulle Ct, Aurora,
CO 80018, United States

IRAQI JOURNAL OF APPLIED PHYSICS LETTERS

ISSN (Print): 1999-656x, ISSN (Online): 2309-1673

INSTRUCTIONS TO AUTHORS

CONTRIBUTIONS

Contributions to be published in this journal should be original research letters, i.e., those not already published or submitted for publication elsewhere, communications or letters to editor.
Manuscripts should be submitted to the editor at the mailing address:

Iraqi Journal of Applied Physics Letters, Editorial Board, P. O. Box 55259, Baghdad 12001, IRAQ
Website: www.iraqiphysicsjournal.com
Email: editor@iraqiphysicsjournal.com, editor_ijap@yahoo.co.uk, ijap.editor@gmail.com

MANUSCRIPTS

Two hard copies with soft Word copy on a CD or DVD should be submitted to Editor in the following configuration:

- **One-column** Double-spaced one-side A4 size with 2.5 cm margins of all sides
- Times New Roman font (16pt bold for title, 14pt bold for names, 12pt bold for headings, 12pt regular for text)
- Manuscripts presented in English only are accepted.
- Total number of words not exceed 2500 words and English abstract not exceed 100 words
- 4 keywords (at least) should be maintained on (PACS preferred)
- Author(s) should express all quantities in SI units
- Equations should be written in equation form (*italic* and symbolic) NOT in plain text
- Tables and Figures should be separated from text and placed in new pages after the references
- Charts should be indicated by the software used for generating them (e.g., Excel, MATLAB, Grapher, etc.)
- Figures and diagrams can be submitted in original colored forms for assessment and they will be returned to authors after provide printable copies
- Only original or high-resolution scanner photos are accepted
- For electronic submission, articles should be formatted with MS-Word software.

AUTHOR NAMES AND AFFILIATIONS

It is IJAPLett policy that all those who have participated significantly in the technical aspects of a paper be recognized as co-authors or cited in the acknowledgments. In the case of a paper with more than one author, correspondence concerning the paper will be sent to the first author unless staff is advised otherwise.
Author name should consist of first name, middle initial, last name. The author affiliation should consist of the following, as applicable, in the order noted:
- Company or college (with department name or company division), Postal address, City, Governorate or State, zip code, Country name, contacting telephone number, and e-mail

REFERENCES

The references should be brought at the end of the article, and numbered in the order of their appearance in the paper. The reference list should be cited in accordance with the following examples:
[1] X. Ning, R. Benford and M.R. Lovell, "On the Sliding Friction Characteristics of Unidirectional Continuous FRP Composites", *J. Tribol. Func. Mater.*, 124(1) (2002) 5-13.
[2] M. Barnes, "Stresses in Solenoids", *J. Appl. Phys.*, 48(5) (2001) 2000–2008.
[3] J. Jones, **"Contact Mechanics"**, Cambridge University Press (Cambridge, UK) (2000), Ch.6, p.56.
[4] Y. Lee, S.A. Korpela and R. Horne, "Structure of Multi-Cellular Natural Convection in a Tall Vertical Annulus", Proceedings of 7th International Heat Transfer Conference, U. Grigul et al., eds., Hemisphere (Washington DC), 2 (1982) 221–226.
[5] M. Hashish, "Waterjet Technology Development", High Pressure Technology, PVP-Vol. 406 (2000) 135-140.
[6] D.W. Watson, "Thermodynamic Analysis", ASME Paper No. 97-GT-288 (1997).
[7] C.Y. Tung, "Evaporative Heat Transfer in the Contact Line of a Mixture", Ph.D. thesis, Rensselaer Polytechnic Institute, Troy, NY (1982).

PROOFS

Authors will receive proofs of papers and are requested to return one corrected copy as a WORD file on a compact disc (CD) or by email. New materials inserted in the original text without Editor's permission may cause rejection of paper unless the handling editor is informed.

COPYRIGHT FORM

Author(s) will be asked to sign the IJAPLett Copyright Form and hence transfer copyrights of the article to the Journal soon after acceptance of it. This will ensure the widest possible dissemination of information.

OFFPRINTS

Authors will receive electronic offprint free of charge and any additional reprints can be ordered.

SUBSCRIPTION AND ORDERS

Annual fees (4 issues per year) of subscription are:
50 US$ for individuals inside Iraq; **200** US$ for institutions inside Iraq;
100 US$ for individuals abroad; **300** US$ for institutions abroad.

Preparation of Cubic Perovskite $CaZnO_3$ Thin Films by Spray Pyrolysis Technique

Raed H. Al-Saqa, Jassim I. K.

Department of Physics, College of Education for Pure Sciences, University of Tikrit, Tikrit, IRAQ

Abstract

Thin films of cubic perovskite ($CaZnO_3$) was deposited using spry pyrolysis deposition (SPD) method. The effect of many precursors concentration on the structural and optical properties of ($CaZnO_3$) thin films have been studied using scanning electron microscope SEM, X-Ray spectrum and UV- spectrum respectively. The transmittance and absorbance of the prepared films with wave length show a clear variation with precursors concentrations, in addition, the energy gap of the films were also varied from 2.7eV to 3 eV. The SEM images and x-ray spectrum of the films shows also clear difference in the shape and structure of the films.

Keywords: Crystal structure; Energy gap; Perovskite; Stability; Thin film
Received: 2 July 2020; **Revised:** 5 September 2020; **Accepted:** 12 September 2020; **Published:** 1 April 2021

1. Introduction

Perovskite materials are considered as a good semiconductor that can replace silicon and germanium. Perovskite has many structures but the most common structure was ABX_3, this structure is made up of five atoms [1] where "A" element has a rather large diameter "B" is a cation of small diameter "transitional or noble metal" [2] and "X" is an oxygen atom and it can be a halogen or a nitrogen [3].

Pervoskite can be easily prepared using several methods such as chemical bath deposition (CBD) [5], chemical vapor deposition (CVD) [6], Silar method [7], spin coating method [8], and spray pyrolysis deposition [9]. Perovskite materials have been used in many industries fields, including capacitors and memories [10], transistors [11], light emitting diodes LEDs [12], measure doses during radiotherapy in x-rays, [13], transparent ceramics [14], photovoltaic cells [15], fuel cells [16] and in the preparation of superconducting materials at relatively high temperatures [17].

In the present study, a different concentration of precursors $ZnCl_2$ and $CaCl_2$ are used to prepare a thin films of inorganic Perovskite structure $CaZnO_3$, the structural properties of these layers were examined using scanning electron microscope (SEM) and x-ray patterns, in addition the transmittance, absorbance, refractive index and extinction coefficient have been also investigated.

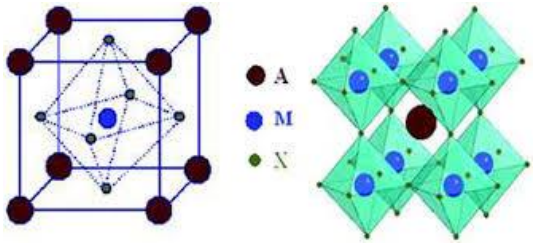

Fig. (1) The perfect stricture of perovskite "ABX_3" which forms a three-sided network"BX_6"[4]

2. Materials and Methods

The films were deposited on glass slides as a substrates. The cleaning process include several steps, they were cleaned ultrasonically using alcohol, methanol, washed by distilled water and finally left to dry. Three different concentrations of $CaCl_2$, $ZnCl_2$ and KOH have been used to prepare thin films of $CaZnO_3$, as in table (1). Each compound was dissolved in 50 ml of distilled water and then the solutions of $CaCl_2$ and $ZnCl_2$ compounds were added simultaneously to KOH solution. The mixture was stirred using magnetic stirrer device for 1hr at 80°C. The later solution was

used to prepare thin films of $CaZnO_3$ on the glass slides at 300°C using spry pyrolysis deposition (SPD). During the deposition process the substrate temperature was kept at 300°C, Atmospheric, pressure 7.5 bar and ten spray steps with period of 5 s.

Table (1) Variation of concentrations of $CaCl_2$, $ZnCl_2$ and KOH

Concentration	$CaCl_2$ (g)	$ZnCl_2$ (g)	KOH (g)
1st	0.8	0.8	0.8
2nd	0.6	0.6	0.8
3rd	0.2	0.2	0.8

3. Results and Discussion

A mixture of different concentration of $ZnCl_2$ and $CaCl_2$ have been used to prepare thin films of $CaZnO_3$ structure, the optical and structural properties of the layers were examined using spectrophotometer, scanning electron microscope (SEM) and x-ray diffraction (XRD) patterns. The optical properties show a clear variation for all concentrations, the transmittance inversely proportional with $ZnCl_2$ and $CaCl_2$ concentration while the absorbance and reflectance decreases. The refractive index spectrum shows a stable value for all concentrations along the range 300-550 nm then decrease over the range 550-600 nm, also the extinction coefficient was inversely proportional with concentration from 300nm to 550nm and then decreases for all concentrations as shown in Fig. (2).

The band gap decreases with increasing concentration, for the first concentration (highest concentration) the energy gap was 2.8 eV then increase to 2.9 eV for the second concentration and finally become 3 eV for the third concentration as in Fig. (2). The variation in the energy gap is due to the continuous changing in the structure and grain size of the films table (2). Scanning electron microscope images of the layers show that the grains size proportional to precursors' concentrations. The image of the first concentration shows the formation of Nano roads structure with diameter of about 90-125 nm, the second concentration image show the formation of a cubic shape grains as a result of the grains aggregation and grow, while the third concentration image show the formation of uniformly distributed grains with size of about 80 nm as in Fig. (2).

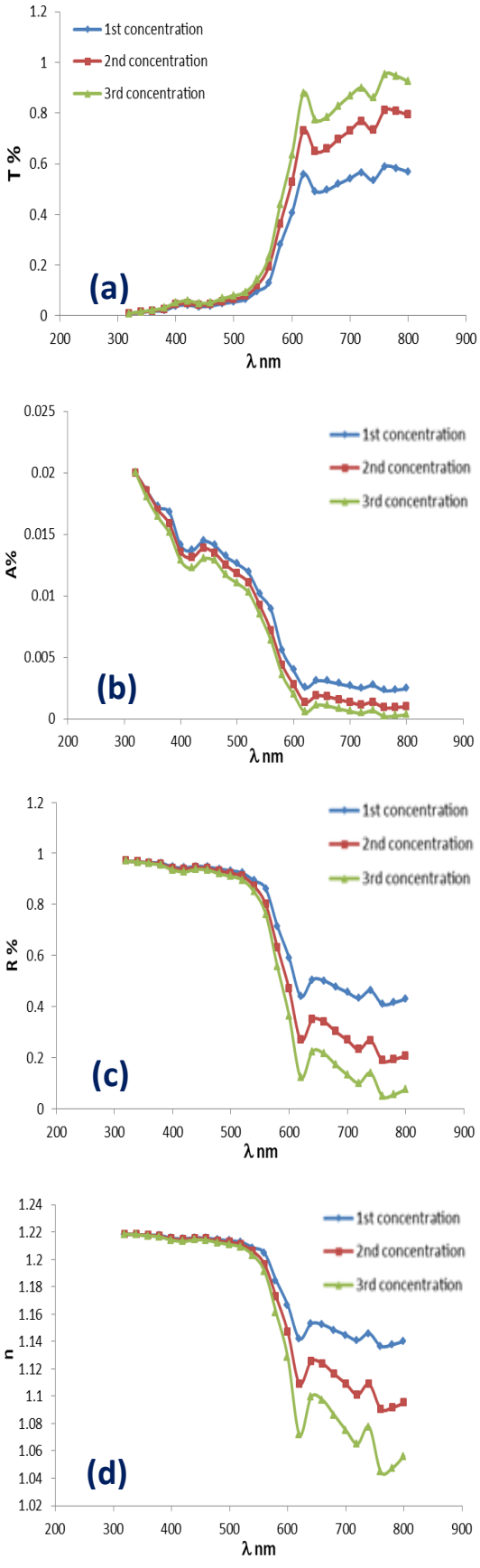

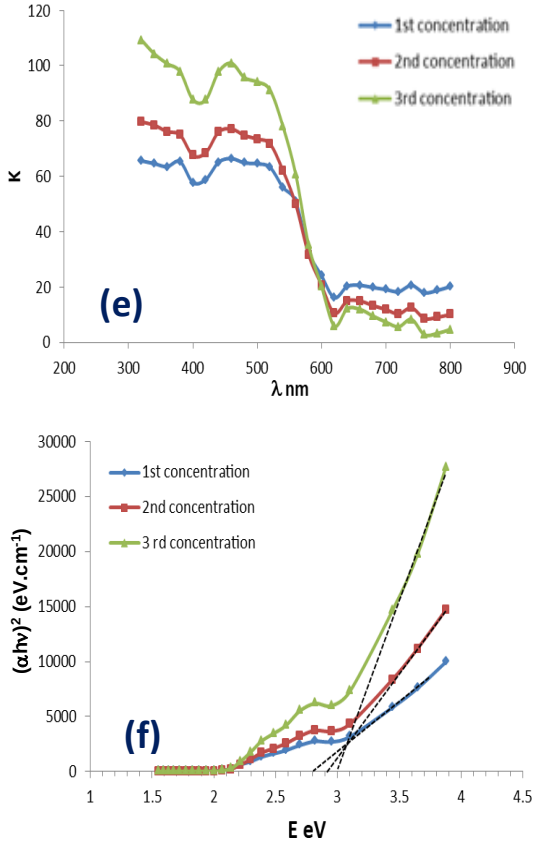

Fig. (2) Effects of concentration on the optical properties: (a) transmission, (b) absorbance, (c) reflectance, (d) refractive index, € extinction coefficient, and (f) energy gap

Table (2) The grain size and energy gap with concentration

Concentration	Average grain size (nm)	Energy gap (eV)
1st	387.4476	2.8
2nd	135.6373	2.9
3rd	88.4817	3

The XRD pattern shows that all the films have amorphous structure with the presence of several peaks belong to the single crystal phase with different intensities at same 2θ in addition to the appearance of another peaks with in the spectrum due to the different orientation in the structure of the prepared films as in Fig. (3).

4. Conclusions

The transmittance, absorbance and reflectance inversely proportional with $ZnCl_2$ and $CaCl_2$ concentration. The refractive index spectrum shows a stable value for all concentrations along the range 300-550 nm then decrease over the range 550-600 nm, also the extinction coefficient decreases for all concentrations. The band gap for the first concentration was 2.8 eV then increase to 2.9 eV for the second concentration and finally become 3 eV for the third concentration. SEM images and for all concentrations show a high variation in the structure of the films. Finally, the results showed the possibility of obtaining a thin film from semiconductor of Pervoskite and therefore can be used in the manufacture of solar cells.

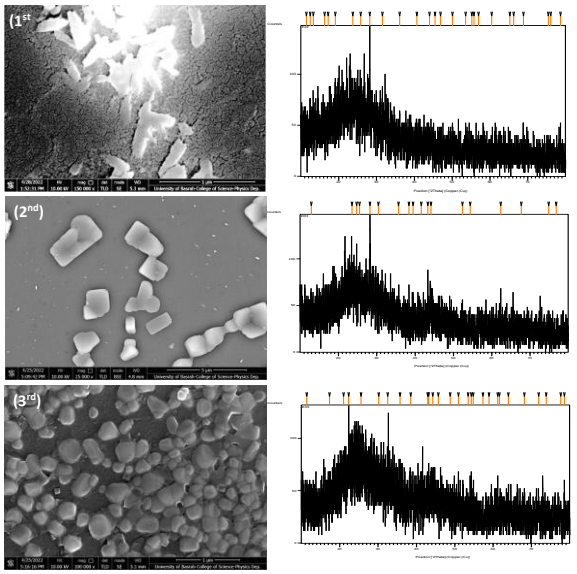

Fig. (3) SEM images and XRD patterns of the layers prepared from different concentrations

References

[1] A. Meziani, "Study of properties structures, electronics, elastics and optics of fluoro-perovskite compounds $CsCdF_3$ and $KZnF_3$", Ph.D. thesis, Badji Mokhtar University, Annaba (Algeria) (2012).
[2] D. Chenine, "Ab-initio study of structural, optoelectronic, thermodynamic and magnetic properties of Perovskite", Ph.D. thesis, Abdelhamid Ibnbadis University, Mostaganem (Algeria) (2019).
[3] K. Jemli, "Synthesis and self-assembly of perovskite molecules for photonics and labeling", Ph.D. thesis, University Paris-Saclay, Paris (France) (2016).
[4] Z. Cheng and J. Lin, "Layered organic–inorganic hybrid perovskites: structure, optical properties, film preparation, patterning and tem-plating engineering", *Cryst. Eng. Comm.*, 12(10) (2010) 2646–2662.
[5] I.A. Younus, A.M. Ezzat and M.M. Uonis, "Preparation of ZnTe thin films using chemical bath deposition technique", *Nanocomp.*, 6(4) (2020) 165-172.
[6] L. Sun et al., "Chemical Vapour Deposition", *Nat. Rev. Methods. Primers*, 1 (2021) 5.
[7] P. Sreedev et al., "Preparation of zinc oxide thin films by SILAR method and its optical analysis", *J.*

Phys.: Conf. Ser., (2019) doi: 1172. 012024. 10.1088/1742-6596/1172/1/012024.
[8] T. Oku et al., "Fabrication and Characterization of CH3NH3PbI3 Perovskite Solar Cells Added with Polysilanes", *Int. J. Photo Energy*, (2018) Article ID 8654963, https://doi.org/10.1155/2018/8654963.
[9] D. Perednis and L.J. Gauckler, "Thin Film Deposition Using Spray Pyrolysis", *J. Electroceram.*, 14 (2005) 103-111.
[10] G. Desgardin, H. Bali and B. Raveau, "Ceramiques composites a base de perovskites et pyrochlores au plomb PZN $(PbZn_{13}Nb_{23})O_3$, PFN $(PbFe_{12}Nb_{12})O_3$ et PMN $(PbMg_{13}Nb_{23})O_3$ pour condensateurs multicouches a haute constante dielectrique", *Mater. Chem. Phys.*, 8(5) (1983) 469-491.
[11] G. Xing et al., "Long-range balanced electron-and hole-transport lengths in organic-inorganic $CH_3NH_3PbI_3$", *Science*, 342 (2013) 344-347.
[12] X. Che, "Theory of halogenated perovskite materials", Ph.D. thesis, University of Rennes 1, Rennes (France) (2018).
[13] G. Murtaza et al., "Elastic and optoelectronic properties of RbMF3 (M= Zn, Cd, Hg): A mBJ density functional calculation", *Physica B: Cond. Matter*, 410 (2013) 131-136.
[14] Ph. Courty et al., "Oxydes mixtes ou en solution solide sous forme très divisée obtenus par décomposition thermique de précurseurs amorphes", *Powder Technol.*, 7(1) (1973) 21-38.
[15] A. Kunioka and Y. Sakai, "Optical and electrical properties of selenium-cadmium sulfide photovoltaic cells", *Solid State Electron.*, 8(12) (1965) 961-965.
[16] N.Q. Minh, "Ceramic fuel cells", *J. Am. Ceram. Soc.*, 76 (1993) 563.
[17] S. Gariglio and J.M. Triscone, "Oxide interface superconductivitySupraconductivité à l'interface d'oxydes", *Compte Rendu Physique*, 12(5-6) (2011) 591-599.

DLS and Zeta Analysis of Biosynthesized Silver Nanoparticles Using Ruta Leaf Extract

Muataz A. Majeed[1], Souad G. Khalil[2], Ghasan A. Naeem[3]

[1] Salahaldeen Education Directorate, Ministry of Education, IRAQ
[2] Department of Physics, College of Science, Baghdad University, Baghdad, IRAQ
[3] Department of Medical Physics, College of Applied Science-Hit, University of Anbar, Hit, Anbar, IRAQ

Abstract

The purpose of this study is to optimize the green synthesis of AgNPs using various quantity of Ruta leaf extracts, the biosynthesized AgNPs were characterized using several methods, UV–visible spectrum, FTIR spectroscopy, DLS and zeta potential. The examination of the visible and ultraviolet spectra revealed an absorption peak in the region of 405-420 nm. Through the use of FTIR spectroscopy, the functional groups that were found in the Ruta plant extract were analyzed in order to locate the components that were accountable for reducing the silver nitrate. X-ray diffraction (XRD), which occurs in the form of (111) lattice planes in the face centered cubic (fcc) structure of metallic silver, the biosynthesized AgNPs were a spherical shape with a nanoscale size ranging between 30-50 nm and moderately stable at -22.53 and -25.88 mV. The preparation resulted in distinct variations in the size of the silver nanoparticles found in the samples. These variations corresponded to the distinct sizes of the extracts employed.

Keywords: Nanotechnology; Ruta leaf; Zeta potential; EDX analysis; Biological method
Received: 3 July 2020; **Revised:** 6 September 2020; **Accepted:** 13 September 2020; **Published:** 1 April 2021

1. Introduction

Phytochemicals in plants, such as polyphenols, flavonoids, tannins, proteins, and sugars, are responsible for synthesizing nanoparticles and serve as reducing and stabilizing agents [1-6]. However, the make-up of these components may be different based on the kind of plant that was extracted, the plant section that was extracted, and the method that was used to extract the plant [7-12]. Because of this, the amount of extract that is used in the reaction has a substantial influence on the technique that is used to prepare the substance [13-15]. When the biological material that is used in the preparation of nanoparticles is increased in concentration, higher contents of the biomolecules that are involved in the process of metal reduction become available [16-19]. This is because the concentration of the biological material is directly proportional to the amount of biomolecules that are present [20,21].

The biogenesis of silver nanoparticles by using ruta leaf extract is the objective of this research. Another objective of this study is to observe the impact of varying the quantity of extract utilized in the manufacture of these particles. Both of these objectives are intended to be accomplished by the end of this study.

2. Materials and Methods

The leaves of the Ruta plant, which were utilized in the production of silver nanoparticles, were obtained from a farm in Kabisa, which is located in Anbar Province in Iraq. The British company Sigma-Aldrich provided silver with a purity level of 99.9%, which was used in the experiment.

After being washed thoroughly with distilled water, the leaves were dried in an electric oven. An electric blender was used to pulverize the dry leaves. To 4 grams of leaf powder, 200 milliliters of distilled water were added. The resulting mixture was heated to 90 degrees Celsius for twenty minutes while being continuously stirred. Whatman filter paper was then used to filter the material that was extracted from the leaves. The extract was stored at a temperature of 3 degrees Celsius until it was required.

the analytical methods that have been used in the process of analyzing the properties of

AgNPs are: Ultraviolet-visible spectroscopy (NOVIALAB, UV-visible 1911 DB spectrometer) was used to investigate the formation of silver nanoparticles in colloidal solution and study the optical properties of the synthesized silver nanoparticles. The zeta potential and nanoparticle distribution were investigated using DLS (Brookhaven Instruments BI-ZTU).

3. Results and discussion

One of the most common approaches of measuring the dimensions of nanoparticles is called dynamic light scattering DLS (Brookhaven Instruments BI-ZTU), which was used in this investigation. The size distribution of silver nanoparticles that were generated using various volumes of extract (0.5, 1 and 1.5 mL) is shown in Fig. (1). the average hydrodynamic size of synthesized AgNPs using Ruta leaf extract was determined to be 103, 89 and 190 nm, respectively with a polydispersity index (PDI). These numerical values for PDI are generally acceptable because the smaller the PDI, the more homogeneous nanoparticles are produced [22].

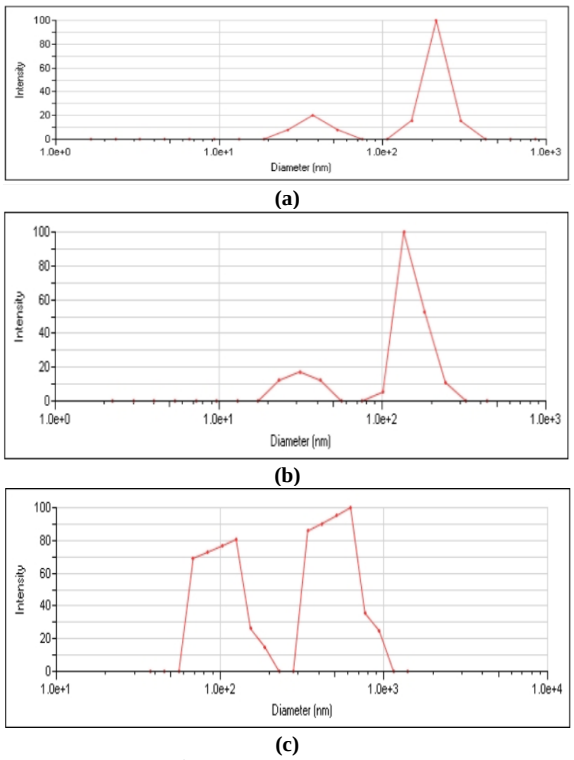

(a)

(b)

(c)

Fig. (1) DLS of AgNPs at (a) 0.5ml (b) 1 ml (c) 1.5ml

One of the most significant aspects that plays a role in shaping the characteristics of nanomaterials is the surface charge of the nanoparticles. The zeta potential of the silver nanoparticles that were generated using varied amounts of extract (0.5, 1 and 1.5 mL) was found to have a charge of -25.88, -22.53, and -23.10 mV, respectively, as shown in Fig. (2). A stable dispersion is indicated without notable AgNPs agglomeration over an extended time in the solution. Previous investigations have stated that nanoparticles with charges in the range of +30mV to −30mV are very stable, and those in the range of +15mV to−25mV are moderately stable [23-25]. As a result of the strong negative repulsion caused by the large negative potential value, AgNPs have an good colloidal nature, are moderately stable over the long term, and have a high dispersion.

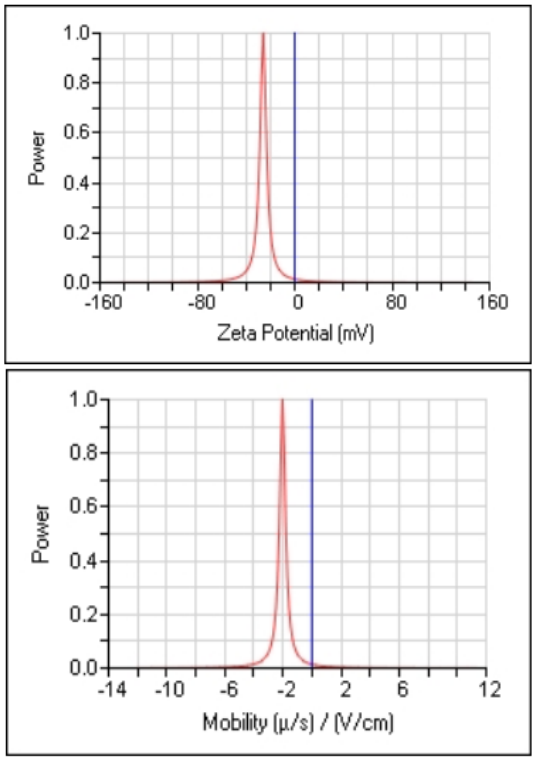

(a)

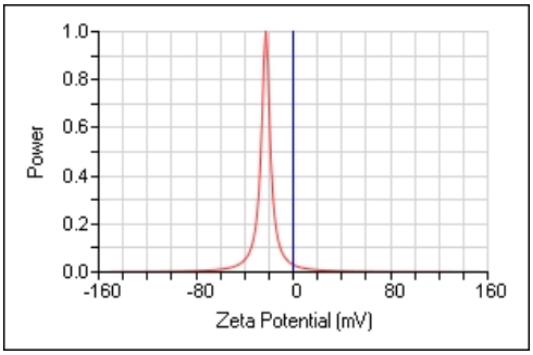

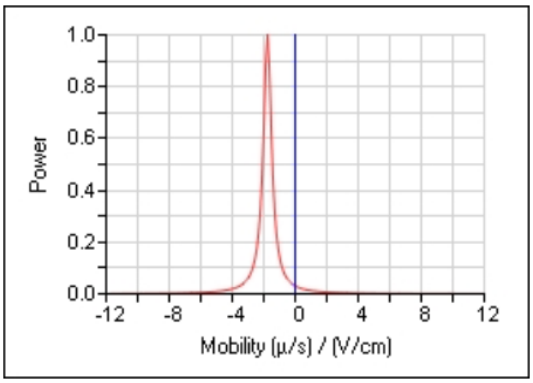

(b)

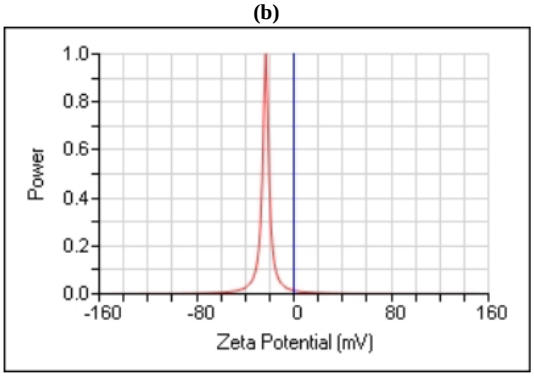

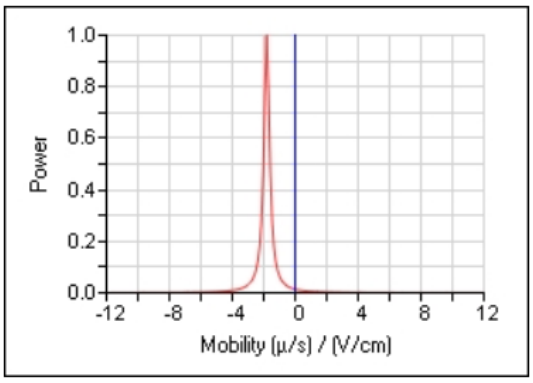

(c)

Fig. (2) Zeta potential of AgNPs at (a) 0.5ml (b) 1 ml (c) 1.5ml

4. Conclusion

Green synthesis of AgNPs using Ruta leaf extract was performed, and AgNPs with well-defined morphologies were created. the results showed that the various quantity of Ruta leaf extracts had substantial effects on the green synthesis of the AgNPs. Based on the results of the current study, the FTIR analysis revealed the presence of some functional groups (O=C-N-H), ($-NH_2$),(-COOH), and (C-O) and confirmed that the bio-compounds: amino acids, proteins, peptides , phenols, amines, carboxylic, and peptides, present in the plant extracts were adsorbed on the surface of the AgNPs, thus enhancing their properties. The different biosynthesized AgNPs are spherical and ranged in size between 30-50 nm and moderately stable. This study focused on the green synthesis of AgNPs using different amounts of rota leaf extracts which induced the formation of AgNPs with well-defined sizes and shapes, thus improving the properties of the nanoparticles.

References

[1] E. Pauwels et al., "Nanoparticles in cancer", *Curr. Radiopharma.*, 1(1) (2008) 30-36.

[2] W.P. Hall, S.N. Ngatia and R.P. van Duyne, "LSPR biosensor signal enhancement using nanoparticle-antibody conjugates", *J. Phys. Chem. C*, 115(5) (2011) 1410-1414.

[3] H. Kato, "In vitro assays: tracking nanoparticles inside cells", *Nature Nanotechnol.*, 6(3) (2011) 139-140.

[4] K. Gudikandula and S. Charya Maringanti, "Synthesis of silver nanoparticles by chemical and biological methods and their antimicrobial properties", *J. Exp. Nanosci.*, 11(9) (2016) 714-721.

[5] M. Ndikau et al., "Green Synthesis and Characterization of Silver Nanoparticles Using Citrullus lanatus Fruit Rind Extract", *Int. J. Anal. Chem.*, 2017, Article ID 8108504.

[6] B.V. Badami, "Concept of green chemistry", *Resonance*, 13(11) (2008) 1041-1048.

[7] J. Kumar Patra and K.-H. Baek, "Green Nanobiotechnology: Factors Affecting Synthesis and Characterization Techniques", *J. Nanomater.*, 2014, Article ID 417305.

[8] H.M.M. Ibrahim, "Green synthesis and characterization of silver nanoparticles using banana peel extract and their antimicrobial activity against representative microorganisms", *J. Rad. Res. Appl. Sci.*, 8(3) (2015) 265-275.

[9] N.W. Mamdooh and G.A. Naeem, "Green Synthesis, Characterization and Biological Activity of Silver Nanoparticles Using Ruta Leaf Extract", *J. Phys.: Conf. Ser.*, 1999, 012050, (2021).

[10] M. Ndikau et al., "Green Synthesis and Characterization of Silver Nanoparticles Using

Citrullus lanatus Fruit Rind Extract", *Int. J. Anal. Chem.*, 2017, Article ID 8108504.

[11] G.A. Naeem et al., "Punica granatum L. mesocarp-assisted rapid fabrication of gold nanoparticles and characterization of nano-crystals", *Enviro. Nanotechnol. Monitor. Manag.*, 14 (2020) 100390.

[12] M.N. Owaid et al., "Synthesis, Characterization and Antitumor Efficacy of Silver Nanoparticle from Agaricus bisporus Pileus, Basidiomycota", *Walailak J. Sci. Tech.*, 17(2) (2020) 75-87.

[13] S.J. Ahmed et al., "Mycosynthesizing and characterizing silver nanoparticles from the mushroom Inonotus hispidus (Hymenochaetaceae), and their antibacterial and antifungal activities", *Enviro. Nanotechnol. Monitor. Manag.*, 14 (2020) 100313.

[14] R.F. Muslim, M.M. Saleh and S.E. Saleh, "Synthesis and characterization of new sulphur six-membered heterocyclic compounds and evaluation their biological activity", *Revista Aus*, 26(2) (2019) 129-135.

[15] S.M. Roopan et al., "Low-cost and eco-friendly phyto-synthesis of silver nanoparticles using Cocos nucifera coir extract and its larvicidal activity", *Ind. Crops Prod.*, 43 (2013) 631-635.

[16] K. Anandalakshmi, J. Venugobal and V. Ramasamy, "Characterization of silver nanoparticles by green synthesis method using Pedalium murex leaf extract and their antibacterial activity", *Appl. Nanosci.*, 6 (2016) 399-408.

[17] N.M. Abd-Alghafour, I.H. Kadhim and G.A. Naeem, "UV detector characteristics of ZnO thin film depositedon Corning glass substrates using low-cost fabrication method", *J. Mater. Sci.: Materials in Electronics*, (2021).

[18] A.N. Ghassan et al., "Green Synthesis of Gold Nanoparticles from Coprinus comatus, Agaricaceae, and the Effect of Ultraviolet Irradiation on Their Characteristics", *Walailak J. Sci. Tech.*, 18(8) (2021) 9396.

[19] E. Gurgur et al., "Green synthesis of zinc oxide nanoparticles and zinc oxide–silver, zinc oxide–copper nanocomposites using Bridelia ferruginea as biotemplate", *SN Appl. Sci.*, 2 (2020) 911.

[20] E.A.M. Hussein et al., "Biologically Synthesized Silver Nanoparticles for Enhancing Tetracycline Activity Against Staphylococcus aureus and Klebsiella pneumonia", *Braz. Arch. Bio. Technol.*, 62 (2019) ??-??.

[21] S.V. Patil et al., "Biosynthesis of silver nanoparticles using latex from few euphorbian plants and their antimicrobial potential", *Appl. Biochem. Biotechnol.*, 167 (2012) 776-790, (2012).

[22] K.N. Nahar et al., "Green synthesis of silver nanoparticles from Citrus sinensis peel extract and its antibacterial potential", *Asian J. Green Chem.*, 5(1) (2021) 135.

[23] V.S. Kotakadi et al., "New generation of bactericidal silver nanoparticles against different antibiotic resistant Escherichia coli strains", *Appl. Nanosci.*, 5(7) (2015) 847-855.

[24] V.S. Kotakadi et al., "Biofabrication and spectral characterization of silver nanoparticles and their cytotoxic studies on human CD34+ve stem cells", *Biotech*, 6(2) (2016) 216.

[25] A.K. Suresh et al., "Monodispersed biocompatible silver sulfide nanoparticles: facile extracellular biosynthesis using the c-proteobacterium, Shewanella oneidensis", *Acta Biomaterialia*, 7(12) (2011) 4253-4258.

Applications of Cold Plasma in Skin Diseases

Hana E. Jasim, Omer W. Mohammed

Department of Physics, College of Science, University of Tikrit, Tikrit, IRAQ

Abstract
Non-thermal atmospheric pressure plasma has recently garnered a lot of attention in the industrial and biological industries because to its numerous benefits, including its high efficiency, straightforward systems, simple operations, non-toxic byproducts, and low cost. In this experiment, argon gas was used to create non-thermal (cold) plasma using a voltage source with a specific frequency (microwave up to 2.4GHz).the discharges of argon gas plasma jet at flow rate (5 L/min) and with voltages (170 V) have been researched to kill some types of bacteria that causes skin diseases.

Keywords: Microwave plasma jet; Bacteria treatment; Plasma parameters; Skin diseases
Received: 4 July 2020; **Revised:** 7 September 2020; **Accepted:** 14 September 2020; **Published:** 1 April 2021

1. Introduction

In the middle of the 20th century, plasma was first created through the interaction of electromagnetic fields with gases like helium or argon. This new generation of electrochemical sources includes microwave plasma (MWP), which operates at a GHz frequency and is particularly useful as an emission source for optical emission spectrometry (OES) and as an ionization source for mass spectrometry (MS). An external cavity or antenna is used to connect the microwave radiation to the gas stream that is going through the torch. According to the mode of power transfer to the plasma gas, the plasma form, and its position relative to the plasma torch, two categories of MWP are often stated. A capacitive linked microwave plasma, initially created by Combine and Wilbur in 1951, is a plasma that resembles a flame at the electrode's tip (CMP). The inner conductor of a CMP torch creates a capacitance against the ground and transmits microwave energy via its tip into the plasma gas. The plasma in the second form is sustained in a quartz or ceramic tube that is housed inside a resonant cavity, where it is created by the inductive transfer of energy from standing waves in a suitable resonator. The term “microwave generated plasma” is frequently used to describe this system (MIP). It is the most effective and widely applied kind of microwave discharge. Either a magnetic field (H pairing) or an electrical field (E pairing) is used to link the microwave energy to the working gas. The usual frequency of a MIP is 2.45 GHz. Seed electrons are introduced into the plasma gas to ignite it, typically, this is done by inserting an electrically conductive and heat-resistant substance while power is being delivered. A correctly tuned system encourages the ionization of the plasma gas following the injection of these seed electrons, and plasma develops. The originally tuned resonant cavity creates a standing electromagnetic wave that is axially oriented to the plasma discharge tube and has a maximum electric field at its center. The cavity is set to have a minimum amount of reflected power after plasma ignition. Exceptionally, under appropriate experimental conditions, heating of the discharge tube and extraction of the seed electrons from the discharge tube material might cause the plasma to ignite "Spontaneously." Flexible working conditions are ensured by a self-ignition of the discharge, which is advantageous, especially when low- In certain MWP sources, nitrogen or air plasmas are created by igniting the plasma with argon while the plasma is being matched to the impedance that is most appropriate for the nitrogen or air discharge. The originally tuned resonant cavity creates a standing electromagnetic wave that is axially oriented to the plasma discharge tube and has a maximum electric field at its center. The cavity is set to have a minimum amount of

reflected power after plasma ignition. Rarely, under particular experimental circumstances immediately following the creation of the argon plasma, the argon flow is progressively replaced by nitrogen or air, allowing for the maintenance of stable plasma in a molecular gas. Different gases, including noble gases, nitrogen, air, oxygen, or carbon dioxide, under both normal and decreased pressure, can produce MWP. The plasma gas's composition and pressure affect the discharge's characteristics. Due to several fundamental differences in the technological design and functioning of these two microwave techniques, the development of CMP and MIP occurred concurrently. A minimum number of charged particles per unit volume is also necessary for the physical description of a plasma, as well as distinctive time and length scales. These factors are connected to the attenuation of the tiny amplitude variations in the plasma's equilibrium state. The variations in space are dampened out over a characteristic length shown by the symbol D. This characteristic distance may alternatively be interpreted as the cancellation of the length scale along the spatial average of electric charge in the plasma. Because the electric fields at distances below LD are local, extremely changeable, and considered microscopic, L>D over the Debye length are typically taken into consideration in plasma physics. The weakly ionized gas in a jet exhaust, for instance, does not meet the criteria for a plasma because the charged particles clash with neutral atoms so often that their motion is governed by regular hydrodynamic forces rather than electromagnetic forces. We need. $\omega\tau > 1$ for the gas to act more like a plasma than a neutral gas if and only if are the frequency and mean duration between collisions with neutral atoms, respectively, of typical plasma oscillations.

2. Experimental Work

Microwave-induced plasma jet system was used. It includes five main parts; microwave source (magnetron), rectangular waveguide, plasma discharge tube, explosion system, gas supply and flow control device. In order to generate microwave radiation with a frequency of 2.45 GHz, a local oven magnetron (Panasonic-2M210) was used and connected to a suitable high voltage circuit (transformer, capacitor and diode). In this experiment, an ionized gas flask is typically an industrial chemical been used in a microwave plasma system. The connection tube between the plasma needle and the gas bottle is installed, and the flowmeter unit that controls the gas passage is l/min. We employ a magnetron attached to the top to produce microwave radiation at a frequency of 2.4 GHz. A voltage circuit that transforms the applied voltage when traveling through a microwave, a component known as a waveguide catches the rays and guides them into a quartz glass tube. By altering the plasma's inherent characteristics, voltage at the input and gas flow rate. For each instance, we investigate how cold plasma affects the inhibition of bacterial growth.

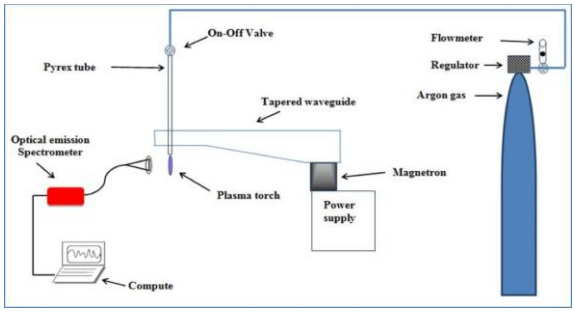

Fig. (1) Diagrammatic drawing of the MIPJ system

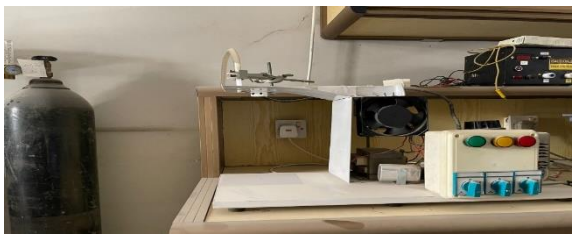

Fig. (2) MIPJ system

3. Results and Discussion

The conditions selected are ; Voltage (170 V), frequency (2.45 GHz), distance (2.5cm), time (15, 30, 60, 180, 300) s and gas flow rates (1, 2, 3, 4, 5) l/min using Microwave plasma jet particularly for this in testing of biomaterials that have undergone plasma

processing and for thorough understanding of the effects of plasma. A plan of attack must be communicated, and medication must be began. Research on destroying bacteria. The percentage of inhibiting and killing bacteria procedure was using a microwave jet plasma and argon gas. We note - through work - how to increase the percentage of inhibition or killing with the increasing of the time used. When exposing a Gram-negative bacteria (pseudomonas), it was found that the bacteria are inhibited with time. At time (15 s) the percentage of bacterial inhibition was (5%), at time (30 s) the percentage of inhibition was (10%), at time (60 s) the percentage of inhibition is (20%), at time (180 s) the percentage of inhibition is (60 %) and at time (300 s) the percentage of inhibition is (100%) as shown in the table (1) above and Fig. (3). The chart below shows that when the exposure time to cold plasma increases the percentage of bacterial inhibition increases with it.

Table (1) The differentiate of number of bacteria with 170V and different time

Voltage (V)	170	170	170	170	170
Time (s)	15	30	60	180	300
Number of bacteria	90	60	35	30	0

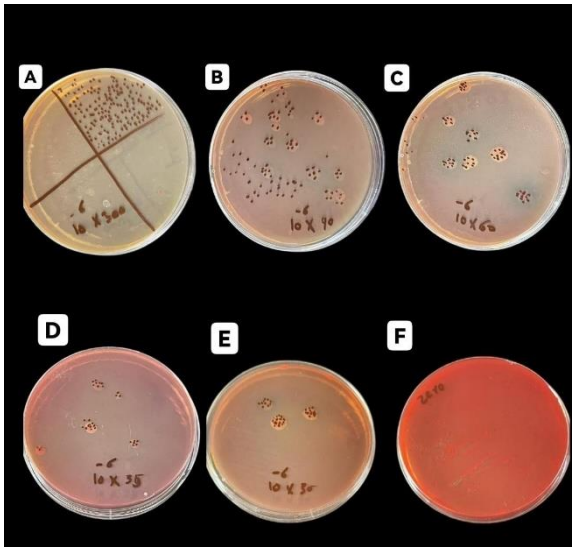

Fig. (3) Pseudomonas growth after exposure to MIPJ plasma system (A: control, B: 15s, C: 30s, D: 60s, E: 180s, F: 300s)

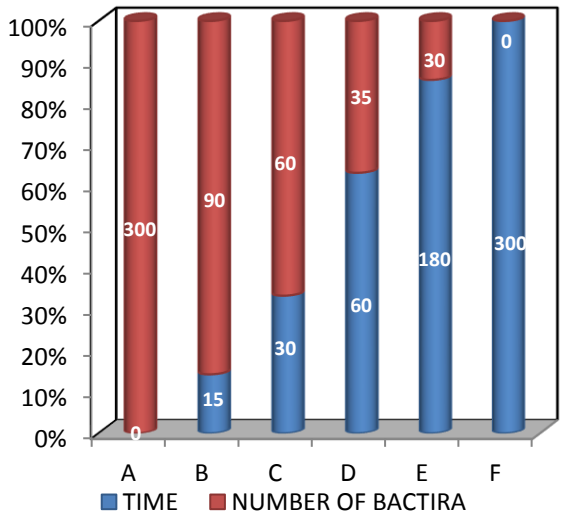

Fig. (4) The ratio between exposure time and bacterial inhibition

The use of low temperature and high pressure plasma in healthcare has created new scientific and technical possibilities. As a result, significant progress has been made in the search for new plasma-based therapies for treatment. A sign that hypothermic plasma may soon be considered an innovative and practical therapeutic in biomedicine and many healthcare related issues. To learn more about upcoming developments in this sector. The reader is provided with references [26, 27]. In fact, it is essential to know how to manage medical emergencies. In this case, plasma apheresis offers a viable alternative to perishable therapies in the form of technology. Undoubtedly, there is still potential for progress in the strategic field of human health regarding the application of plasma processes. Especially for this in the testing of biomaterials that have undergone plasma treatment and a comprehensive understanding of the effects of plasma. The action plan must be reported and treatment initiated. To decide when plasma therapy should be given, he should follow vital clinical signs before and after exposure.

4. Conclusions

The results indicate that as the duration of exposure to cold plasma increases, so does the rate of bacterial inhibition, which is important for the development of plasma-based therapies for wound healing, cancer treatment

and other clinical specialties. We anticipate significant developments in bio-oriented knowledge in plasma science and technology in the near future, and firmly believe that relevant plasma-based therapeutic approaches will be developed at that time, and will have a significant impact on human health care from fundamental, clinical and economic.

References

[1] M. Yousfi et al., "Analysis of ionization wave dynamics in low-temperature plasma jets from fluid modeling supported by experimental investigations", Plasma Sources Sci. Technol., 21 (2012) 045003.

[2] S.J. Kim et al., "Characteristics of multiple plasma plumes and formationof bulletsin an atmospheric-pressure plasma jet array", IEEE Trans. Plasma Sci., 43(3) (2015) 753759.

[3] R. Zhang et al., "Plasma jet array treatment to improve the hydrophobicity of contaminated HTV silicone rubber", Plasma Sci. Technol., 19(10) (2017) 105505.

[4] D.J. Jin, H.S. Uhm and G. Cho, "Influence of the gas-flow reynoldsnumber on a plasma column in a glass tube", Phys. Plasmas, 20(8) (2013) 083513.

[5] J.R. Ferrell et al., "Characterization, Properties and Applications of Nonthermal Plasma: A Novel Pulsed-Based Option", J. Biotechnol. Biomater., 3 (2013) ??-??.

[6] J.P. Boeuf, L. Yang and L. Pitchford, "Dynamics of guided streamer (plasma bullet) in a helium jet in air at atmospheric pressure", J. Phys. D: Appl. Phys., 46 (2013) 015201.

[7] Y.A. Lebedev, "Microwave discharges: generation and diagnostics", in IOP J. Phys.: Conf. Ser., 257(1) (2010) 012016.

[8] A. Begum, M. Laroussi and M.R. Pervez, "Atmospheric pressure helium/air plasmajet: breakdown processes and propagation phenomenon", AIP Adv., 3 (2013) 062117.

[9] G.B. Stretenovic et al., "Spatio-temporally resolved electric field measurements in helium plasma jet", J. Phys. D: Appl. Phys., ? (2014) ??-??.

[10] A.M. Lietz and M.J. Kushner, "Electrode configurations in atmospheric pressure plasma jets: production of reactive species", Plasma Sources Sci. Technol., 27 (2018) 105020.

[11] J. Winter, R. Brandenburg and K.D. Weltmann, "Atmospheric pressure plasma jets: an overview of devices and new directions", Plasma Sources Sci. Technol., 24 (2015) 054001.

[12] D.J. Jin, H.S. Uhm and G. Cho, "Influence of the gas-flow Reynolds number on a plasma column in a glass tube", Phys. Plasmas, 20(8) (2013) 083513.

[13] H.R. Metelmann, T. von Woedtke and K.D. Weltmann, **"Comprehensive Clinical Plasma Medicine"**, Springer (Berlin, 2018).

[14] K.D. Weltmann et al., "The future of plasma science and technology", Plasma Process. Polym., 16 (2019) e1800118.

[15] R. Jover et al., "Optimization of MnO_2/Vertically Aligned Carbon Nanotube Composite for Supercapacitor Application", J. Power Sources, 196 (2011) 5779-5783.

[16] A.M. Lietz and M.J. Kushner, "Molecular admixtures and impurities in atmospheric pressure plasma jets", J. Appl. Phys., 124 (2018) 153303.

[17] A.J. Mohamed, M.K. Khalaf and A.S. Jasim, "The Study of the Characteristics of a Microwave Plasma Jet Operated with Ar at Atmospheric pressure", *Tikrit J. Pure Sci.*, 27(4) (2022) 70-76.

[18] X. Lu et al., "Reactive species in non-equilibrium atmospheric pressure plasma: generation, transport, and biological effects", Phys. Rep., 630 (2016) 1-84.

[19] L. Conde, "An Introduction to Plasma Physics and its Space Applications", Ph.D. thesis, Universidad Politecnica, Madrid (Spain, 2014) 6-7.

[20] R. Zhang et al., "Plasma jet array treatment toimprove the hydrophobicity of contaminated HTV silicone rubber", Plasma Sci. Technol., 19(10) (2017) 105505.

[21] N. Barekzi and M. Laroussi, "Fibropblasts cell morphology altered by low temperature atmospheric pressure plasma", IEEE Trans. Plasma Sci., 42 (2014) 2738.

[22] S. Mohades et al., "Evaluation of the effectsof a plasma activated mediumon cancer cells", Phys. Plasmas., 22 (2015) 122001.

[23] N. Barekzi and M. Laroussi, "Effects of low temperature plasmas on cancer cells", Plasma Process. Polym., 10 (2013) 1039.

[24] S. Toyokuni et al., **"Plasma Medical Science"**, Cambridge Academic Press (MA, 2018).

[25] S. Mohades, N. Barekzi and M. Laroussi, "Efficacy of low temperature plasmaagainst scaber cancer cells", Plasma Process. Polym., 11 (2014) 1150-55.

[26] A.J. Mohamed, "A study on the properties of a microwave plasma diffuser Al atmospheric pressure and using argon and air gases and hetium to remove microbial contamination", Tikrit University (2022) ?????

[27] S. Bekeschus et al., "White paper on plasma formedicine and hygiene: future in plasma health sciences", Plasma Process. Polym., 16 (2019) e1800033.

Output Power of Si-CNT Solar Cell Fabricated by Plasma Sputtering Technique

Zahraa B. Ibraheem[1], Mohammad M. Uonis[1], Mazin A. Abed[2]

[1] Department of New and Renewable Energy, College of Science, Mosul University, Mosul, IRAQ
[2] Department of Physics, College of Science, Mosul University, Mosul, IRAQ

Abstract
Plasma sputtering technique was used to deposit carbon layers with different nanoscale thicknesses on p-type silicon wafers. The scanning electron microscope images showed that the grains size grow and aggregate in a cluster. The electrical properties of the junction behave as a solar cell and this gave proof of the formation of carbon nanotubes. The out power and efficiency of the Si-CNT cells increases with carbon layer thickness and light intensity.

Keywords: Carbon nanotubes; Solar cells; Heterojunction; Cold plasma
Received: 5 July 2020; **Revised:** 8 September 2020; **Accepted:** 15 September 2020; **Published:** 1 April 2021

1. Introduction

The importance of carbon as a chemical element comes from the ability of its large atoms to bond with each other or with atoms of different chemical elements in different ways. This diversity in bonding gives a diversity of structural forms, including crystalline carbon such as graphite and fullerene, amorphous carbon and carbon nanoparticles, including carbon nanotubes, each of these shapes is characterized by different properties, including a low coefficient of friction, high thermal conductivity, optical transmittance, hardness, as well as being non-toxic or harmful to the environment. In 1985, Kroto and Smalley gave the name fullerene to clusters of carbon atoms that contain sixty carbon atoms C_{60}, which are a group of icosahedral symmetry closed molecules and because of the similarity between them and Buckminster's designs R. Buckminster has been called 'buckminster fullerene', and for short these molecules are called 'buckyball' [1,2]. Fullerene particles have attracted great interest in recent research because of their distinct electrical and mechanical properties, including high electrical conductivity, hardness, and others. Fullerene molecules are the basis for the construction of carbon nanotubes, because the ends of the carbon nanotubes are in the form of fullerene molecules [3]. Each carbon atom in the fullerene is aligned with three other carbon atoms and the positions of the carbon atoms in the fullerene molecule (C_{60}) are identical and are located at a fixed distance from the center of the molecule (approximately 3.55Å) and the average distance between each Two adjacent carbon atoms of 1.44 Å and the fullerene (C_{60}) can be counted as a coiled graphite layer that generates a symmetric polyhedral shape consisting of 20 hexagonal rings and 12 pentagonal rings needed to form curved surfaces and this agrees with Euler's theorem. The carbon nanotubes are originally bi-directional strips of graphene wrapped around a specific axis to form a cylindrical shape with a diameter ranging between (50-0.4 nm), each carbon atom hybrid (sp^2) has three covalent bonds With three other carbon atoms, and the fourth electron is in un hybridized orbital π and since the unit cell in graphene includes two atoms, there will be even numbers of electrons that can give the conductor or semiconductor properties of carbon nanotubes [4]. Different techniques have been used in the preparation of carbon nanotube such as hot-filament (HF-CVD) [5-7], thermal chemical vapor deposition [8,9], plasma-enhanced chemical vapor deposition (PECVD) [10,11], and laser ablation technique [12,13].

In this study, different thickness of carbon nano layers (30.5, 52.6 and 70.12 nm) have

been used in the preparation of Si-CNT solar cell, carbon layers were examined using Scanning electron microscope and measure the effect of the layer thickness and light intensity on the solar cell out power.

2. Experimental Method

Carbon nano layers have been deposited on silicon wafers to prepare Si-CNT junction using plasma sputtering technique. The impurities expected to be formed on the surface of silicon strips can be divided into three categories, contamination fills, discreet particles and absorbed gas atoms as a result of processing silicon strips during the preparation. In the process of cleaning the silicon wafers, chemical compounds are used as solvents for removing different types of impurities, and it includes a set of successive steps in which the silicon wafers is washed with distilled water for 2-3 minutes, washed with ethanol solution by ultrasonic for a period of 5-10 minutes, washed with distilled water for 2-3 minutes, washed with ultrasonic acetone solution for 5-10 minutes, washed with distilled water for 2-3 minutes and then immersed in hydrofluoric acid (HF) at a concentration of 9% for one minute to remove a layer of silicon dioxide generated as a result of oxidation, washed with distilled water for 2-3 minutes and finally immersed in acetone solution in order for the model to be dried directly [14,15]. The plasma atomization technique was used to deposit a layer of carbon with different thicknesses (30.5, 52.6 and 70.12 nm) of pure graphite columns (99.9%) in a vacuum chamber of 10-2 mbar in an atmosphere of argon gas, the device used in the plasma atomization process is Q150R S/E/ES shown in Fig. (1).

The device-specific variables are determined by which the thickness and structure of the carbon deposited layer can be controlled according to the amount of current passing through the carbon column, the time of the pulses and the number of pulses as shown in table (1). Gold was used as the electrode for the Si-CNT junction, layers of gold were deposited on the top and back surfaces of the junction to measure the electrical properties as shown in Fig. (2). The variables used in gold deposition are shown in table (2).

Table (1) Values of variables used in carbon deposition

Parameter	Value
Material	Carbon
Pulse Current	70 A
Pulses Length	10 s
Number of Pulses	5
Out Gas Time	60 s
Out Gas Current	50 A

Table (2) Values of variables used in gold deposition

Parameter	Value
Material	Gold
Sputter Current mA	70 A
Terminate thickness (nm)	70 nm
Tooling factor	5
Out Gas Time	30 second
Out Gas Current	50 A

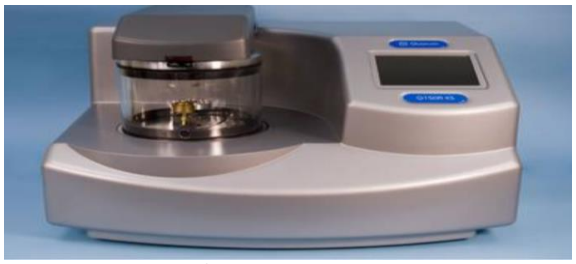

Fig. (1) Photograph of the Q150R S/E/ES plasma atomization system

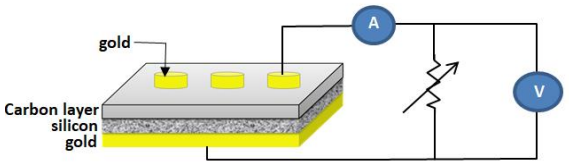

Fig. (2) Sample structure and the circuit used for measurement

3. Results and Discussion

Silicon wafers (p-type) have been used as a substrate to deposit different thickness of carbon nano layers (30.5, 52.6 and 70.12 nm) in the preparation of silicon-carbon nanotube junction (Si-CNT), the effect of the layer thickness and light intensity on the solar cell out power were investigated.

The effect of thickness on the Si-CNT solar cell shown in Fig. (5), the out power of the Si-CNT junction (at a constant light intensity 60W) increases with carbon layer thickness. The efficiency also increases with carbon layer thickness from 0.3 for the carbon layers with thickness 30.5 nm to 0.87 for the carbon layers with thickness 52.6 nm and then the efficiency become 1.45 for the carbon layers

with thickness 70.12 nm, this increase in efficiency with the thickness of the carbon layer could be due to the increase in the density of the carbon nanotubes as shown in table (3).

thickness nm	power	I_{sc} μA	V_{oc} mv	I_{max} μA	V_{max} mv	FF	η
30.5	60	18.2	17.2	12.7	14.2	0.576093	0.300566921
	40	13.1	13	10	8.4	0.493247	0.13999994
	20	9.8	9.3	6.3	7.2	0.497696	0.075600022
52.6	60	28.1	28.55	24.5	21.4	0.653533	0.873833528
	40	22.1	23.5	17.3	15.6	0.51965	0.449800379
	20	17.3	20.2	12.5	12.1	0.432811	0.252083553
70.12	60	37.5	38.55	28.5	30.6	0.603268	1.453498838
	40	28.1	33.9	24	19.8	0.498851	0.79200079
	20	24	28.2	17	15.5	0.389332	0.439166496

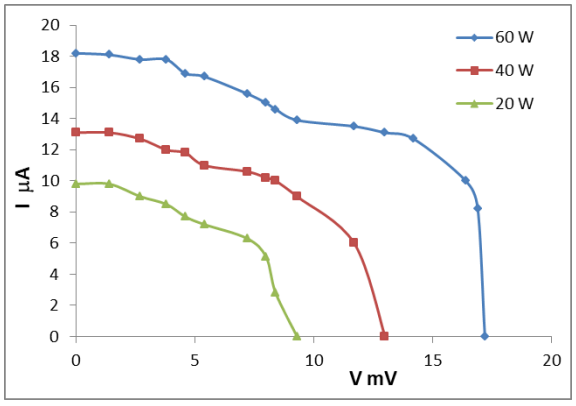

(a)

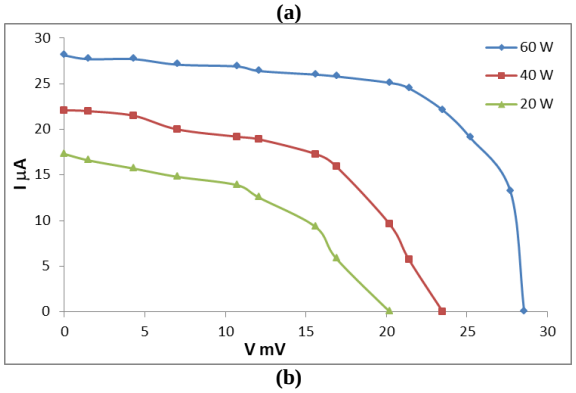

(b)

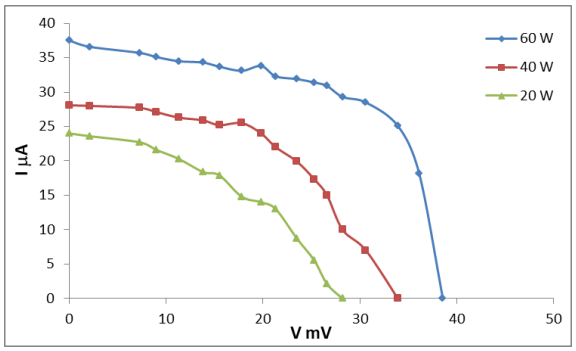

(c)

Fig. (4) Out power of the Si-CNT solar cells with different carbon light intensities (20,40 and 60W) and layers thicknesses (a) 30.5 nm, (b) 52.6 nm, and (c) 70.12 nm

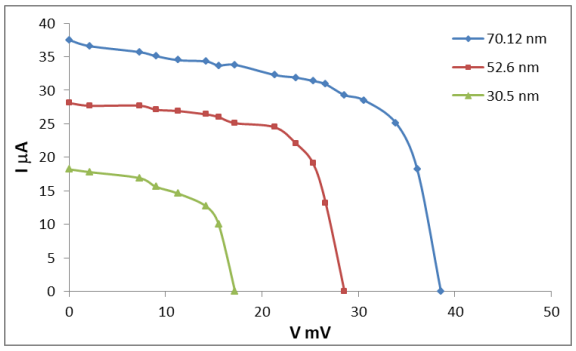

Fig. (5) The out power of Si-CNT solar cell with different carbon layer thickness

4. Conclusions

The carbon nanotubes have been constructed on a p-type silicon wafer substrates without catalysts. Scanning electron microscope showed that the grain size increases slightly with layer thickness. The Si-CNT junction behave as a solar cell, the out power and efficiency increases with carbon layer thickness and light intensity.

References

[1] Timothy D. Burchell, (1999), "*Carbon Materials for Advanced Technologies*" 1st Edition, Elsevier Science Ltd the Boulevard, Langford Lane Kidlington, Oxford 0x5 IGB, UK.

[2] Andreas Hirsch, (2010) "The era of carbon allotropes", Nature Materials, VOL 9, pp.868-871, Macmillan Publishers Limited, www.nature.com/naturematerials.

[3] Pradeep T., (2007) "*Nano:the essential, understanding the nanoscience and nanotechnology* ", Tata McGraw-Hill Publishing Company Limited, New Delhi.

[4] Daniel Jay Hornbaker, (2003) "Electronic Structure of Carbon Nanotube Systems Measured with Scanning Tunneling Microscopy", Ph.D. thesis, Physics in the Graduate College of the

University of Illinois at Urbana-Champaign, Urbana, Illinois.

[5] Edward H. Wahl, (2001) "Laser-Based Diagnostics Of Diamond Synthesis Reactors", Report No. TSD-136, The U.S. Department of Energ Basic Energy Sciences, Stanford University Stanford, California 94305-3032.

[6] Ganesh E.N., (2013) " Single Walled and Multi Walled Carbon Nanotube Structure, Synthesis and Applications", International Journal of Innovative Technology and Exploring Engineering (IJITEE) Volume-2, Issue-4, March 2013, pp.311-320.

[7] Farabaugh E.N., A. Feldman, and L. Robins, (1991) "Influence of Filament Geometry on Hot Filament Growth of Diamond Films ", 2nd Internation Conference on the Now Diamond Science and Technology, National Institute of Standards and Technology Ceramics Division Gathersburg, MD 20899.

[8] Jurg F., (2006) "Growth of Single-Wall Carbon Nanotubes by Chemical Vapor Deposition for Electrical Devices", Ph.D. thesis, Philosophisch-Naturwissenschaftlichen, Universitat Basel.

[9] Daenen M.,R.D. de Fouw,B. Hamers,P.G.A. Janssen,K. Schouteden, M.A.J. Veld, (2003) "The Wondrous World of Carbon Nanotubes 'a review of current carbon nanotube technologies'", Phillips NAT-lab, Eindhoven University of Technology.

[10] Andrea Szabó, Caterina Perri, Anita Csató, Girolamo Giordano, Danilo Vuono 2 and János B. Nagy, (2010) " Synthesis Methods of Carbon Nanotubes and Related Materials", Materials, 3, 3092-3140. www.mdpi.com/journal/materials.

[11] Todd Steiner, (2004) "*Semiconductor Nanostructures for Optoelectronic Applications*", Artech House, Inc., Boston, London, International Standard Book Number:1-58053-751-0.

[12] Scott C.D., S. Arepalli, P. Nikolaev, R.E. Smalley, (2001)" Growth mechanisms for single-wall carbon nanotubes in a laser-ablation process", Materials Science & Pocessing,Appl. Phys. A72, 573–580.

[13] Muhammad Musaddique, Ali Rafique, Javed Iqbal, (2011) "Production of Carbon Nanotubes by Different Routes— A Review ", Journal of Encapsulation and Adsorption Sciences, 1, 29-34.

[14] Werner Kern, (1990) " The Evolutionof Silicon Wafer Cleaning Technology ", J. Electrochem. Soc., Vol. 137, No. 6, pp.1887-1891.

[15] Virginia Semiconductor, Inc., (2003) "Wet-Chemical Etching and Cleaning of Silicon",www.virginiasemi.com, tech@virginiasemi.com.

[16] Mohammad M. Uonis, Bassam M. Mustafa, Anwar M. Ezzat (2014) " The Role of Sputtering Current on the Optical and Electrical Properties of Si-C Junction " World Journal of Nano Science and Engineering,4, 90-96.

[17] Mohammad M. Uonis, Bassam M. Mustafa, Anwar M. Ezzat (2014) " The Effect of Carbon Rod-Specimens Distance on the Structural and Electrical Properties of Carbon Nanotube ", World Journal of Nano Science and Engineering, 4, 105-110

[18] Dresselhaus M. S., G. Dresselhaus, and R. Saito, (1995) "Physics of Carbon Nanotubes", Carbon, Vol. 33, No. 7, pp. 883-891.

Structural Properties for Cadmium Oxide Nanostructures Prepared by Plasma Jet Technique

Omar A. Gadaan[1], K. H. Razyg[1], Kadhim A. Aadim[2]

[1] Department of Physics, College of Education for Pure Sciences, Tikrit University, IRAQ
[2] Department of Physics, College of Science, University of Baghdad, Baghdad, IRAQ

Abstract
In the present study, cadmium oxide nanoparticles have been prepared from bulk structure by the induced plasma technique at different bombardment times. These nanoparticles were prepared as thin layers on glass substrates with different thicknesses (prepared at different times of shelling). After that, they were analyzed with a UV-visible spectrophotometer, Scanning electron microscope SEM, atomic force microscope AFM and X-ray spectrum. When the optical properties and their constants were measured, the energy gap of the films increased in the range of 2.94-3.2 eV with bombardment times. The examining images of AFM and SEM show a clear variation in the structure where the roughness varies with bombardment time due to the variation in the nanoparticles' diameter. Finally, the x-ray spectrum shows that the layers are completely crystalline.

Keywords: Cadmium oxide; Nanoparticles; Plasma jet, Optical properties; Structural properties
Received: 6 July 2020; **Revised:** 9 September 2020; **Accepted:** 16 September 2020; **Published:** 1 April 2021

1. Introduction

Cadmium oxide is soluble in acids only while it is insoluble in water and alkalis [1]. It is one of the (II-VI) group compounds and has a cubic crystal structure with face-centered (FCC) unit cells similar to the structure of a crystal of sodium chloride (NaCl) (Fig. 1) [2-4]. Cadmium oxide. It is a semiconductor material within the group of transparent conductive oxides (TCO) and has distinct properties, including a relatively large energy gap range of 2.2–2.7 eV. [5-7], transparency in the visible region Near infrared rays (NIR) [8,9], high reflectivity in the red region of the electromagnetic spectrum [10,11], high mobility of carriers [12], high electrical conductivity similar to the conductivity of negative-type metals (n-type) [3,8], and has good fluorescence, cadmium oxide has many applications such as electro-optical devices [13], phototransistors [14], biological and catalytically applications [15], and gas sensors [16]. Several techniques have been used in the preparation of cadmium oxide thin films, such as magnetron sputtering [17,18], sol gel method [19] and spray pyrolysis technique [20].

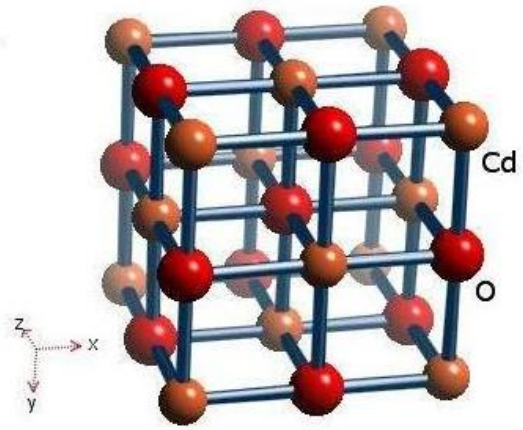

Fig. (1) A diagram of the CdO crystal structure [16]

2. Preparation Method

Solutions containing nanoparticles were prepared by the induced plasma deposition method for different preparation periods 4, 6, 8, 10 min. Cadmium metal foils 99% purity have been used as a source for cadmium. The cleaning of the foils was carried out using polishing paper and then washed with ethanol alcohol to remove any impurities present on the surface of the metals.

The cadmium metal before placing it in the glass beaker had dimensions of length and width of about 10 cm^2, after that, a part of the cadmium metal was cut to about 1.5 cm^2, it will be immersed in a 10 ml glass beaker

containing 7 ml of distilled water. The nozzle of the needle is directed in the middle of the metal. If a needle nozzle is located at a distance of 7 cm^2 from the target, then in order to generate a spark in the form of a scattered blue flame, the metal foil will be connected to the positive electrode while the negative electrode will be connected to the needle nozzle. The process will be carried out in the presence of argon gas that flows at a constant rate (3 L/s).

3. Results and Discussion

The cadmium oxide CdO particles have been prepared using the plasma-jet technique for different preparation periods (bombardment) in the range of 4, 6 8, and 10 min. The surface roughness is also decreases with bombardment time table (1).

Table (1) AFM measurements and energy gap for the prepared samples at various bombardment times

Bombardment time (min)	Surface thickness (nm)	Roughness average (nm)
4	74.75	7.491
6	43.27	8.00 9
8	10.04	5.150
10	7.678	1.059

X-ray diffraction patterns in Fig. (2) show that the layers are extremely crystalline with cubic structure for all bombardment periods, the peaks for all periods appear with small differences in 2θ and small differences in intensities, which is reflected in the calculated grain size, the grain size decreases with bombardment period as in table (2), and this agree with AFM images shown in Fig. (3). Also, SEM images show that the grain size decreases with bombardment time as shown in Fig. (4), and this agree with x-ray and AFM measurements.

Table (2) Average grain size for different bombardment time

Bombardment time	Average grain size
4 min	5.4
6 min	4.9
8 min	3.9
10 min	3.5

Table (3) Energy band gap of the CdO prepared at different bombardment periods

bombardment time (min)	Energy gap (eV)
4	2.94
6	3.1
8	2.96
10	3.2

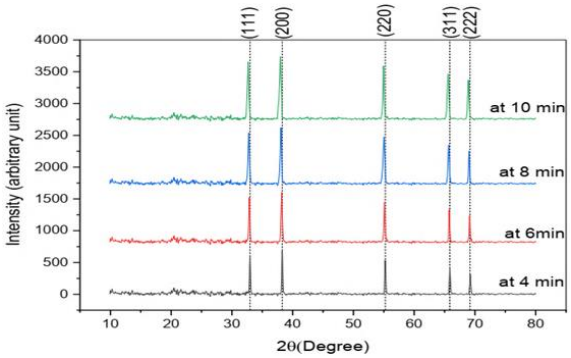

Fig. (2) XRD patterns of CdO metal oxide after preparing it with induced plasma bombardment with different times

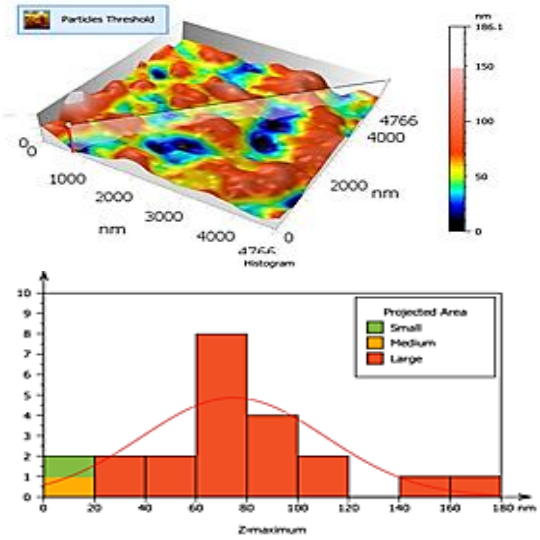

4 min

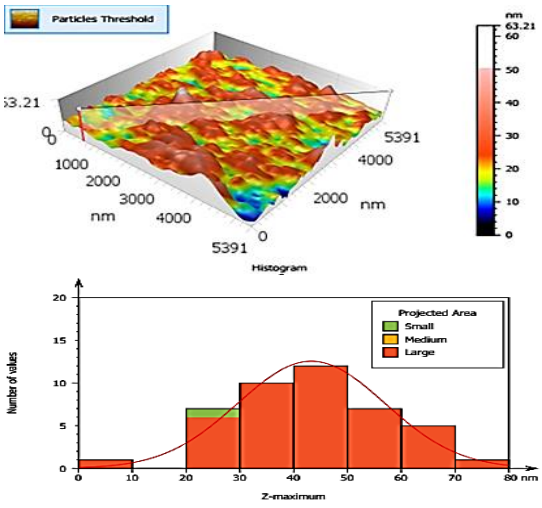

6 min

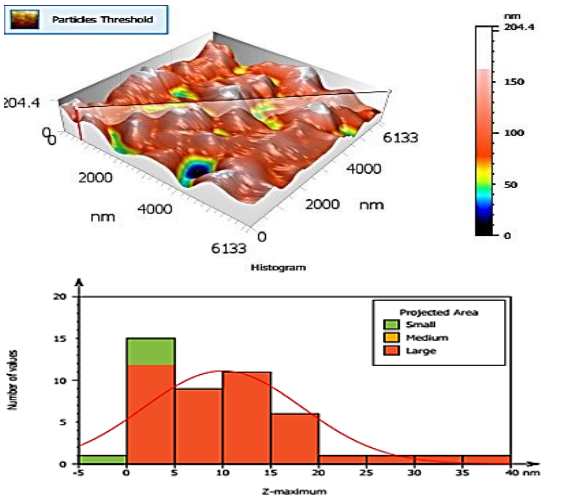

8 min

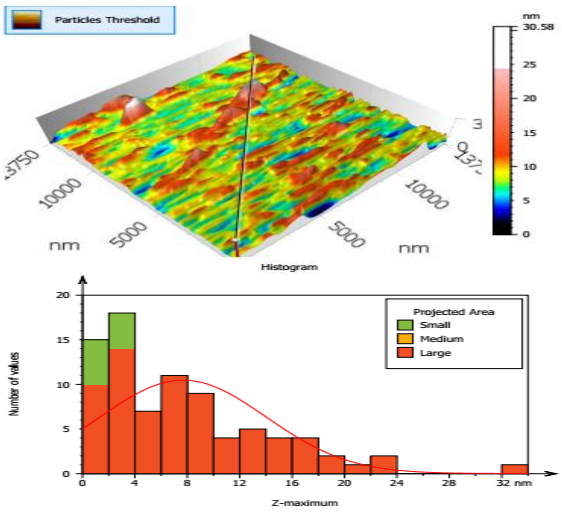

10 min

Fig. (3) Structural properties of CdO after plasma-get bombardment for different bombardment periods (4, 6, 8 and 10) min

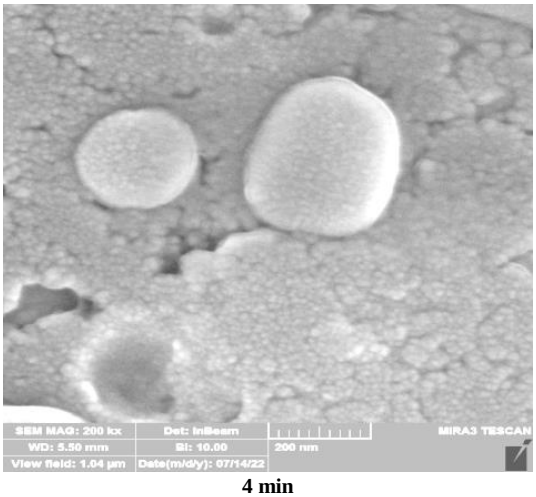

4 min

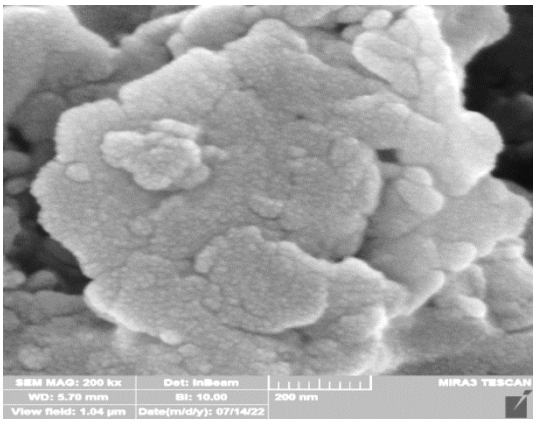

6 min

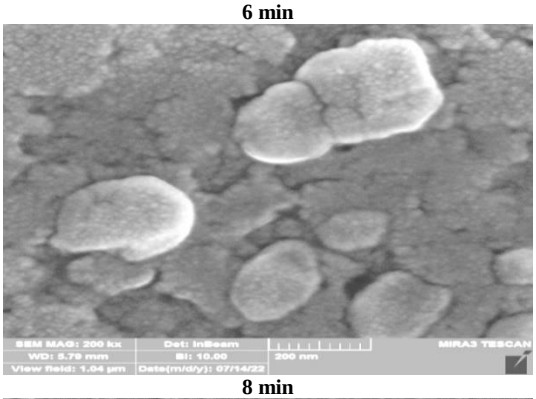

8 min

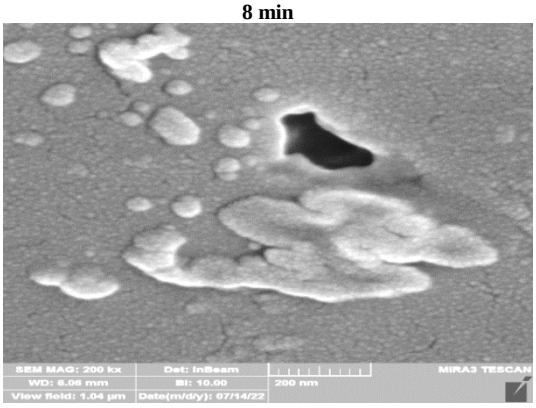

10 min

Fig. (4) SEM images of CdO prepared at different bombardment periods (4, 6, 8 and 10) min

4. Conclusions

Cadmium oxide nanoparticles have been prepared using the plasma-Get technique for different bombardment periods. AFM images show that the roughness and surface thickness decrease with bombardment periods, and this agrees with SEM images and the X-ray spectrum. The X-ray spectra show that the layers are completely crystalline. The peaks for all periods appear at the same 2θ with different intensities. In addition, the calculated grain size decreases with periods from 5.4 to 3.5 nm. The optical properties and energy gap varied clearly with bombardment periods.

References

[1] P. Pradyot, **"Handbook of Inorganic Chemicals"**, Mc Graw-Hill, Inc., (2003)152.

[2] C.H. Bhosale et al., "Structural, optical and electrical properties of chemically sprayed CdO thin films", Mater. Sci. Eng. B, 122 (2005) 67–71.

[3] T. Ghoshal, S. Kar and S. Chaudhuri, "Synthesis of nano and micro crystals of $Cd(OH)_2$ and CdO in the shape of hexagonal sheets and rods", Appl. Surf. Sci., 253 (2007)7578–7584.

[4] A.A. Dakhel and A.Y. Ali-Mohamed, "Structural, electrical, and optical absorption properties of $La_xCd_{1-x}O$ solid solution films obtained by sol–gel method, Mater. Chem. Phys., 113(2009)356–360.

[5] S. Ilican et al., "CdO:Al films deposited by sol–gel process: a study on their structural and optical properties", Optoelectron. Adv. Mater.: Rapid Commun., 3(2) (2009) 135-140.

[6] D.M. Carballeda-Galicia et al., Thin Solid Films, 105 (2000) 371.

[7] Y. Caglar, S. Ilican and M. Caglar, "Single-oscillator model and determination of optical constants of spray pyrolyzed amorphous SnO_2 thin films", Eur. Phys. B, 58(3) (2007) 251-256.

[8] A.A. Dakhel, "Influence of hydrogenation on the electrical and optical properties of CdO:Tl thin films", Thin Solid Films, 517 (2008) 886–890.

[9] A. Badawi et al., "Tailoring the optical properties of CdO nanostructures via barium doping for optical windows applications", Phys. Lett. A, 411 (2021).

[10] Y. Zhang and J. Mu, "Preparation of CdO Thin Films by Annealing Cd^{+2}-Dithiol Self-Assembled Films", Disper. Sci. Technol., 26 (2005) 509–511.

[11] M. Uonis, B. Mustafa and A. Ezzat, "The Role of Sputtering Current on the Optical and Electrical Properties of Si-C Junction", World J. Nano Sci. Eng., 4 (2014) 90-96.

[12] X. Li et al., "High Mobility CdO Films and Their Dependence on Structure", Solid-State Lett., 4 (2001) 66-68.

[13] A.A. Dakhel and A.Y. Ali-Mohamed, "Structural and optoelectrical properties of nanocrystalline Gd-doped CdO films prepared by sol gel method", Sol-Gel Sci. Technol., 55 (2010) 348–353.

[14] R.K. Gupta et al., "Wide band gap $Cd_{0.83}Mg_{0.15}Al_{0.02}O$ thin films by pulsed laser deposition", Appl. Surf. Sci., 255 (2009) 4466-4469.

[15] Z. Zhao, D.L. Morel and C.S. Ferekides, "Electrical and optical properties of tin-doped CdO films deposited by atmospheric metalorganic chemical vapor deposition", Thin Solid Films, 413 (2002) 203-211.

[16] S.M. Sze, **"Physics of Semiconductor Devices"**, John Wiley and Sons (NY, 1986).

[17] K.H. Mahmoud, Z.M. El–Bahy and A.I. Hanafy, "Photoluminescence analysis of Er nanoparticles in cadmium–phosphate glasses", J. Non-Cryst. Solids, 363 (2013) 116–120.

[18] A.M. Mostafa et al., "Synthesis of Cadmium oxide Nanoparticles by Pulsed laser ablation in liquid environment", Int. J. Light Electron Opt., 144 (2017) 679-684.

[19] B. Goswami and A. Choudhury, "Enhanced visible luminescence and modification in morphological properties of Cadmium oxide Nanoparticles induced by annealing", J. Exp. Nanosci., 10(12) (2014) 900-910.

[20] K. Viswanathan and F.C. Bor, "Synthesis and characterization of poly(N–vinylpyrrolidine)–silica hybrid shell coated cadmium selenide/cadmium sulphide and cadmium selenide/zinc sulfde nanoparticles", Mater. Lett., 65(4) (2011) 646–649.

Laser-Induced Breakdown Spectroscopy of Nickel Plasma

Huda H. Abbas, Sabah N. Mazhir

Department of Physics, College of Science for Women, University of Baghdad, Baghdad, IRAQ

Abstract

In this research, the optical emission spectrometry (OES) technique was used to record the spectrum resulted from the plasma generated from a (Ni) target in the air by using of a Q- switched Nd:YAG laser with a wavelength of 1064nm, a pulse duration of 10ns, a focal length of 10cm, and a repetition rate of 6Hz in the energy range 300-500mJ. Plasma parameters such as temperature, electron density, Debye sphere length, and plasma frequency were calculated using the Boltzmann-Plot and Stark broadening method. The resulting spectrum of plasma was recorded with different energy values. The results of the plasma parameters resulting from the laser showed that their values increased with increasing energy, and the electron temperature was ranging between 0.934 and 1.479eV.

Keywords: Optical emission spectrometry (OES); Laser-induced breakdown spectroscopy; Plasma
Received: 8 July 2020; **Revised:** 15 September 2020; **Accepted:** 22 September 2020; **Published:** 1 April 2021

1. Introduction

Laser induced breakdown spectroscopy (LIBS) is based on the laser plasma atomic emission spectroscopy, is a kind of spectroscopy that has been developed [3,4]. As a novel method of matter element analysis, it possesses some of advantageous characteristics, including high resolution, nearly nondestructive measurement of the target, the ability to analyze multiple elements in real-time online at the same time, and the ability to be applied to solid, liquid, gas, and aerosol materials. LIBS is capable of achieving both qualitative and quantitative analysis of the target material, and as a result, the technique is extensively used in environmental pollution monitoring, diamond jewelry evaluation, and industrial manufacturing. In addition to laser properties such as wavelength, pulse energy, and pulse width; the nature of the target material and the surrounding environment; as well as the measuring equipment, all of these factors may impact LIBS [5-7]. As a result of these factors, the repeatability of the LIBS signal is low, which is one of the key challenges that plague the deployment of LIBS technology [8,9]. The study of hardware improvement, as well as research into the system through experiment equipment, measurement environment, optimizing target material properties, and other methods of improving the accuracy of experimental data has been conducted to overcome matrix effects and improve the accuracy of experimental data. It has thus become a significant research trend to increase the dependability and stability of LIBS technology by improving the spectrum of data processing, as a result of these considerations [10-11]. The purpose of this research is to evaluate the effects of laser energy on plasma emissions as well as the characterization of Ni plasmas in air.

2. Experimental LIBS Setup

Figure (1) shows a schematic diagram of the experimental setup in this work. It depicts a schematic of the LIBS experimental setup. The tests were carried out at room temperature and pressure. Nickle samples were chosen for plasma production, and the goal purity was nearly 99.9999 percent. With a Q-switched nanosecond laser source, which has an essential wavelength of 1064 nm, a pulse duration of 10 ns, and a repeating frequency of 6 Hz, the plasma was generated. Analysis of the spectrometer's optical emission was done. The distance from the spectrometer to the laser target is around 30 cm. The laser-induced plasma light emissions from the Ni

target surface were captured using an optical fiber with a 50 µm diameter core that was positioned at a 1 cm distance. NIST database software [12] was used to calibrate the optical emission line to specified elements to determine the plasma properties.

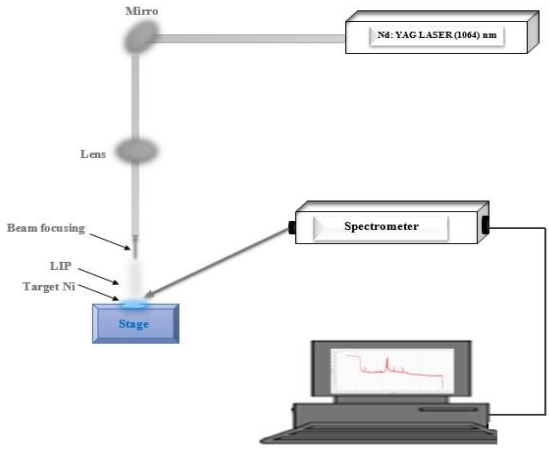

Fig. (1) Schematic diagram of the experimental setup for LIBS

3. Results and Discussion

Spectra of Ni plasma produced by LIBS. Figure (2) depicts the radiation spectrum of Ni plasma at wavelengths ranging from 200 nm to 1000 nm in wavelength. As may be seen in Fig. (2), several nickel emission lines (such as Ni I at 286.55, 366.40, 385.83, 440.15, 446.24, 460.5, 471.57, 485.54, 508.40 and 547.08 nm, among others) are superimposed over continuous background radiation. Ni I emission lines include 286.55 and 366.40 nm. The collision of plasma particles between bremsstrahlung and electronics-ion compound radiation has been shown experimentally and theoretically to be the primary source of the strong background radiation in the early plasma [1,2]. The generation time and attenuation rate of continuous background radiation, ionizing radiation, and atomic radiation, on the other hand, are all distinct. Because of the delay in the formation of the plasma, the background intensity will decrease fast, and atomic radiation and ionizing radiation will progressively get stronger and narrower as the time delay progresses [13]. The correlation data of the atomic spectral standard and the technical database from the National Institute of Standards and Technology (NIST) as well as spectral line analysis software from the spectrometer were used to identify the nickel atom spectrum in Fig. (2).

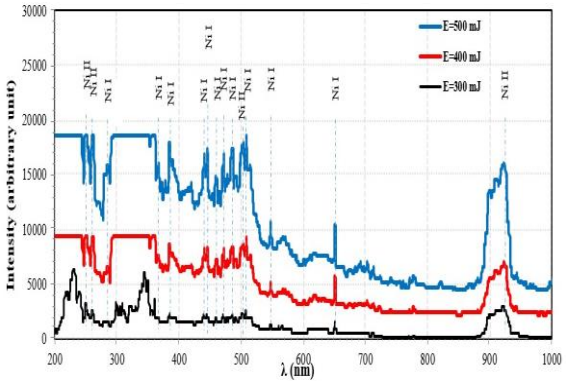

Fig. (2) Nickel plasma within the spectral range 200-1000nm

Laser-induced Ni plasma electron temperature measured with a laser beam. In plasma, the electron temperature and the electron density are two fundamental thermodynamic characteristics that must be considered. Only when the plasma is under Local Thermodynamic Equilibrium circumstances does the temperature of the plasma have physical relevance (LTE) [13]. When the plasma is in LTE, the electron temperature may be used to define the key plasma properties. For example, in the LTE, particle velocities are distributed by the Maxwell distribution, while particle numbers in different energy levels are distributed in accordance with the Boltzmann distribution. The adjacent ionization state of a single particle is distributed in accordance with the Saha distribution. As predicted by the Boltzmann distribution of particles, the spectral line intensity Iji and the spectral energy Ej associated with the higher level are both met in the following ways [14].

$$\ln\left[\frac{I_{ji}\,\lambda}{hc\,g_j\,A_{ji}}\right] = -\frac{1}{kT_e}\,E_j + \ln\left[\frac{N}{4\pi\,U}\right] \quad (1)$$

For each level, A_{ji} denotes the transition probability, gj indicates the statistical weight of the higher level, h denotes The Planck constant, and c denotes the speed of light in a vacuum. E_j the energy at the top level, in this equation, T_e is the temperature of the electrons, k is the Boltzmann constant, U is a partition function, and N is the total number density of species, all in degrees Celsius.

It is possible to obtain the plasma temperature without knowing N or U if the vertical coordinate is $\ln\left[\frac{I_{ji}\,\lambda}{hcg_j\,A_{ji}}\right]$ and the horizontal coordinate is Ej, and the Boltzmann diagram is fitted in a linear manner. If the Boltzmann diagram is fitted in a linear manner, a line with a slope of $-\frac{1}{kT_e}$ is obtained. When attempting to solve the plasma electron temperature problem, it is necessary to know the excitation energy of the upper- level E_j, the degeneracy of the upper energy level g_j, and the spontaneous transition probability of the spectral lines A_{ji}, among other things. It has been shown that the literature estimates of the likelihood of spontaneous emission transition of the spectral lines A_{ji} are significantly different and that the measurement error of the spectral line intensity E_j is quite substantial. As a result, the estimated plasma temperature of electrons will have a large inaccuracy, which will result in poor precision for the other plasma characteristics.

Table (1) Physical characteristics of NI, NII lines

Space	Wavelength (nm)	$A_{ji}.g_j$	E_i eV	E_k eV
Ni II	251.08	5.8 E8	1.68	6.61
Ni II	261.5	5.40E+06	1.68	6.39
Ni I	286.55	9.00E+06	0.21	4.53
Ni I	366.4	6.00E+06	0.27	3.65
Ni I	385.83	4.80E+07	0.42	3.63
Ni I	440.15	4.20E+08	3.19	6
Ni I	446.24	8.50E+07	3.46	6.24
Ni I	460.5	1.60E+08	3.47	6.17
Ni I	471.57	1.40E+08	3.54	6.17
Ni I	485.54	2.80E+08	3.54	6.09
Ni II	506.42	5.20E-03	1.15	3.6
Ni I	508.4	2.80E+08	3.67	6.11
Ni I	547.69	2.80E+07	1.82	4.08
Ni I	653.28	6.30E+04	1.93	3.82
Ni II	937.48	6.20E-05	0	1.32

As a result of advancements in the iterative Boltzmann technique, it is now possible to measure the electron temperature of laser coin-induced plasma. Because of the correlation coefficient of linear fitting of 0.6529 and the Boltzmann diagram (Fig. 3) of the nickel atom line shown in Eq. (1), the electron temperature of the plasma in Ni is determined to be 10829.07 K as shown in Fig. (4). The linear correlation coefficient of the line hits 0.8356 after 600 mJ laser energy of the Boltzmann method, according to the flow chart (Fig. 5). In other words, based on the slope found above, the electron temperature of the Ni plasma is 15993.29K. Ni plasma's electrical temperature remains constant between 15993.29 and 10829.07 K throughout experimentation, increasing the linear fitting coefficient (Fig. 6a and 6b) from 0.6529 to 0.8356. Table (1) lists the physical properties of the N I and N II lines the technical database from the National Institute of Standards and Technology (NIST) employed in this experiment.

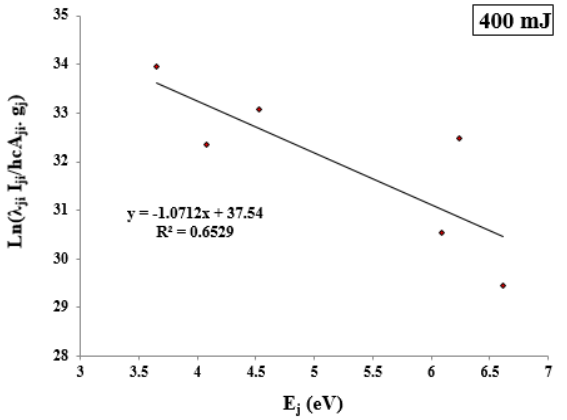

Fig. (3) A Boltzmann plot of 400 mJ Ni I emission lines with a correlation coefficient of R^2 0.6529

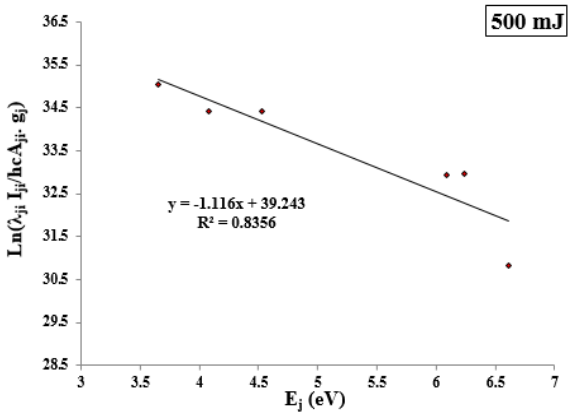

Fig. (4) A Boltzmann plot of 500 mJ Ni I emission lines with a correlation coefficient of R^2 0.8356

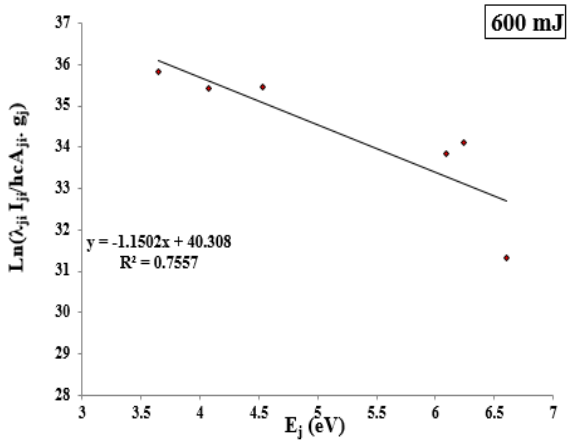

Fig. (5) A Boltzmann plot of 600 mJ Ni I emission lines with a correlation coefficient of R^2 0.7557

4. Conclusion

Using optical emission spectroscopy (OES), the plasma spectra of the pulsed Q-switched Nd:YAG laser incident were examined on a Ni target in air at a fundamental wavelength of 1064 nm. The spectra of the plasma showed multiple emission lines from the element Ni. The irradiance of the laser was used to model the plasma and estimate its characteristics. The higher the power of the laser, the higher the temperature of the electrons and the higher the density of the electrons. In addition to this, the plasma frequency, Debye length, and number all rose as the laser light strength increased. The findings also shown that the plasma is heated to a greater degree whenever there is interaction between the laser and the plasma.

References

[1] M. Burger, M. Skočić and S. Bukvić, "Study of self-absorption in laser induced breakdown spectroscopy", *Spectrochimica Acta Part B: Atom. Spectro.*, 101 (2014) 51-56.

[2] D.A. Cremers and L.J. Radziemski, **"Handbook of Laser-Induced Breakdown Spectroscopy"**, *John Wiley & Sons, Ltd.* (Chichester, 2006).

[3] M.L. Najarian and R.C. Chinni, "Temperature and Electron Density Determination on Laser-Induced Breakdown Spectroscopy (LIBS) Plasmas", *A Phys. Chem. Exp., J. Chem. Educ*., 90(2) (2013) 244–247.

[4] S.A.M. Mansour, "Self-absorption effects on electron temperature-measurements utilizing laser induced breakdown spectroscopy (LIBS) techniques", *Opt. Photon. J.*, 5 (2015) 79-90.

[5] A.S. Al-Aamer and A.M. El-Sherbini, "Measurement of Plasma Parameters in Laser-Induced Breakdown Spectroscopy Using Si-Lines", *WJNSE*, 2(4) (2012) 206-212.

[6] H.A. Yuan et al., "Investigation of laser-induced plasma at varying pressure and laser focusing", *Spectrochimica Acta, Part B Atom. Spectro*., 150 (2018) 33-37.

[7] S. Hafeez, N.M. Shaikh and B. Rashid, "Plasma properties of laser-ablated strontium target", *J. Appl. Phys.*, 103(8) (2008) 083117(1-8).

[8] K.A. Yahya and B.F. Rasheed, "Effects of Discharge Current and Target Thickness in Dc - Magnetron Sputtering on Grain Size of Copper Deposited Samples", *Baghdad Sci. J*., 16(1) (2019) 84-87.

[9] S. N. Mazhir et al., "Effects of Gas Flow on Spectral Properties of Plasma Jet Induced by Microwave", *Baghdad Sci. J.*, 15(1) (2018) 81-86.

[10] N. Naeema, A. Kudher and G. Mohammed, "Study of the Spectroscopic Performance of Laser Produced CdTe, and CdTe:Ag Plasma', *IOP Conf. Ser.: Mater. Sci. Eng*., 757 (2020) 012025.

[11] N.K. Abdalameer and S.N. Mazhir, "Laser-Induced Plasma Atomic and Ionic Emission during Target Ablation", *Int. J. Nanosci.*, 20(5) (2021) 1–8.

[12] National Institute of Standards and Technology. *Atomic spectra database* [DB/OL] (2017).

[13] S.N. Mazhir et al., "A Study of Plasma parameters in gold sputtering System by Means of Optical Emission Spectroscopy", *IOP Conf. Series: Mater. Sci. Eng.*, 871 (2020) 012081.

[14] K.A. Aadim et al., "Influence of Gas Flow Rate on Plasma Parameters Produced by a Plasma Jet and its Spectroscopic Diagnosis Using the OES Technique", *IOP Conf. Ser.: Mater. Sci. Eng*., 987 (2020) 012020.

[15] S.A.M. Mansour, "Self-Absorption Effects on Electron Temperature-Measurements Utilizing Laser Induced Breakdown Spectroscopy (LIBS)-Techniques", *Opt. Photon. J.*, 5 (2015) 79-90.

[16] M. Fikry, W. Tawfk and M. Omar, "Investigation on the effects of laser parameters on the plasma profle of copper using picosecond laser induced plasma spectroscopy", *Opt. Quantum Electron*., 52 (2020) 249.

[17] W.L. Wiese, J.R. Fuhr and A. Lesage, "Experimental Stark Widths and Shifts for Spectral Lines of Neutral and Ionized Atoms (A Critical Review of Selected Data for the Period 1989 through 2000)", *J. Phys. Chem. Ref. Data*, 31(3) (2002) 819-927.

IRAQI JOURNAL OF APPLIED PHYSICS LETTERS
EDITORIAL BOARD

COPYRIGHT RELEASE FORM

IRAQI JOURNAL OF
APPLIED PHYSICS LETTERS (IJAPLett)

We, the undersigned, the author/authors of the article titled

……
……
……
……
……
……
……

that is submitted to the Iraqi Journal of Applied Physics Letters (IJAPLett) for publication, declare that we have neither taken part or full text from any published work by others, nor presented or published it elsewhere in any other journal. We also declare transferring copyrights and conduct of this article to the Iraqi Journal of Applied Physics Letters (IJAPLett) after accepting it for publication.

The authors will keep the following rights:

1. Possession of the article such as patent rights.
2. Free of charge use of the article or part of it in any future work by the authors such as books and lecture notes after informing IJAP editorial board.
3. Republishing the article for any personal purposes of the authors after taking journal permission.

To be signed by all authors:

Signature:……..date: ……
Printed name: ……

Signature:……..date: ……
Printed name: ……

Signature:……..date: ……
Printed name: ……

Correspondence author:……...
……
Address:……
……
Telephone:……..……..email: ……

Note: Complete and sign this form and mail it to the below address with your finally revised manuscript

The Iraqi Journal of Applied Physics Letters
ISSN (Print): 1999-656x, ISSN (Online): 2309-1673
www.iraqiphysicsjournal.com
Email: editor@iraqiphysicsjournal.com
Email: editor_ijap@yahoo.co.uk
Email: ijap.editor@gmail.com

IRAQI JOURNAL OF APPLIED PHYSICS LETTERS
Volume (4) Issue (2) April-June 2021

CONTENTS

The *Iraqi Journal of Applied Physics Letters (IJAPLett)* is a peer reviewed journal of high quality devoted to the publication of original research papers from applied physics and their broad range of applications. IJAPLett publishes quality original research letters in physics and its applications in the broadest sense. It is intended that the journal may act as an interdisciplinary forum for physics and its applications. Innovative applications and material that brings together diverse areas of physics are particularly welcome. IJAPLett aims to disseminate knowledge; provide a learned reference in the field; and establish channels of communication between academic and research experts, policy makers and executives in industry, commerce and investment institutions. IJAPLett is a quarterly specialized periodical dedicated to publishing original letters in: Applied & Nonlinear Optics, Applied Mechanics & Thermodynamics, Digital & Optical Communications, Electronic Materials & Devices, Laser Physics & Applications, Plasma Physics & Applications, Quantum Physics & Spectroscopy, Semiconductors & Optoelectronics, Solid State Physics & Applications, Alternative & Renewable Energy, and Environmental Science & Technology.

Sponsored and Published by
Iraqi Society for Alternative and Renewable Energy Sources and Techniques

Co-published by
American Quality for Scientific Publishing